

On Sparse High-Dimensional Graphical Model Learning For Dependent Time Series

Jitendra K. Tugnait

Abstract—We consider the problem of inferring the conditional independence graph (CIG) of a sparse, high-dimensional stationary multivariate Gaussian time series. A sparse-group lasso-based frequency-domain formulation of the problem based on frequency-domain sufficient statistic for the observed time series is presented. We investigate an alternating direction method of multipliers (ADMM) approach for optimization of the sparse-group lasso penalized log-likelihood. We provide sufficient conditions for convergence in the Frobenius norm of the inverse PSD estimators to the true value, jointly across all frequencies, where the number of frequencies are allowed to increase with sample size. This results also yields a rate of convergence. We also empirically investigate selection of the tuning parameters based on Bayesian information criterion, and illustrate our approach using numerical examples utilizing both synthetic and real data.

Index Terms—Sparse graph learning; graph estimation; time series; undirected graph; inverse spectral density estimation.

I. INTRODUCTION

Graphical models are a useful tool for analyzing multivariate data [1], [2], [3]. A central concept is that of conditional independence. Given a collection of random variables, one wishes to assess the relationship between two variables, conditioned on the remaining variables. In graphical models, graphs are used to display the conditional independence structure of the variables.

Consider a graph $\mathcal{G} = (V, \mathcal{E})$ with a set of p vertices (nodes) $V = \{1, 2, \dots, p\} = [p]$, and a corresponding set of (undirected) edges $\mathcal{E} \subset [p] \times [p]$. Given a (real-valued) random vector $\mathbf{x} = [x_1 \ x_2 \ \dots \ x_p]^T$, in the corresponding graph \mathcal{G} , each variable x_i is represented by a node (i in V), and associations between variables x_i and x_j are represented by edges between nodes i and j of \mathcal{G} . In a conditional independence graph (CIG), there is no edge between nodes i and j if and only if (iff) x_i and x_j are conditionally independent given the remaining $p - 2$ variables. Gaussian graphical models (GGM) are CIGs where \mathbf{x} is real-valued multivariate Gaussian. Suppose \mathbf{x} has positive-definite covariance matrix $\Sigma (= \mathbb{E}\{\mathbf{x}\mathbf{x}^T\})$ with inverse covariance matrix (also known as precision matrix or concentration matrix) $\Omega = \Sigma^{-1}$. Then Ω_{ij} , the (i, j) -th element of Ω , is zero iff x_i and x_j are conditionally independent [1]–[3].

Graphical models were originally developed for random vectors with multiple independent realizations, i.e., for time

series that is independent and identically distributed (i.i.d.). Such models have been extensively studied [4]–[8]. Graphical modeling of real-valued time-dependent data (stationary time series) originated with [9], followed by [10]. Time series graphical models of i.i.d. or dependent data have been applied to intensive care monitoring [11], financial time series [12]–[15], social networks [16], air pollution data [10], [13], analysis of EEG [17]–[19], and fMRI (functional magnetic resonance imaging) data [14], [20], [21], colon tumor classification [22] and breast cancer data analysis [23]. A significant technical issue in these analyses and applications is that of model selection. Given p nodes in V , in an undirected graph, there are $p(p-1)/2$ distinct edges. Which edges are in \mathcal{E} , and which are not – this is the model selection (graph learning) problem.

In a dependent time series GGM \mathcal{G} , edge $\{i, j\} \in \mathcal{E}$ iff time series components $\{x_i(t)\}$ and $\{x_j(t)\}$ are conditionally dependent. In [10] the term “partial correlation graph” is used for such graphs. A key insight in [10] was to transform the series to the frequency domain and express the graph relationships in the frequency domain. Denote the power spectral density (PSD) matrix of $\{\mathbf{x}(t)\}$ by $\mathbf{S}_x(f)$, where $\mathbf{S}_x(f) = \sum_{\tau=-\infty}^{\infty} \mathbf{R}_{xx}(\tau) e^{-j2\pi f\tau}$, the Fourier transform of $\mathbf{R}_{xx}(\tau) = \mathbb{E}\{\mathbf{x}(t+\tau)\mathbf{x}^T(t)\}$. In [10] it was shown that conditional independence of two time series components given all other components of the time series, is encoded by zeros in the inverse PSD, that is, $\{i, j\} \notin \mathcal{E}$ iff the (i, j) -th element of $\mathbf{S}_x^{-1}(f)$, $[\mathbf{S}_x^{-1}(f)]_{ij} = 0$ for every f . This paper is concerned with sparse high-dimensional graphical modeling of dependent time series. It is noted in [10] that for partial correlation graph estimation via nonparametric methods, checking for $[\mathbf{S}_x^{-1}(f)]_{ij} \equiv 0$ is computationally much less demanding than using time-domain methods where one would need to calculate $2\binom{p}{2}$ linear filters (see [10, p. 161] for details). Therefore, in this paper we focus on frequency-domain methods, particularly for high values of series dimension.

A. Related Work

Prior work on graphical modeling for dependent time series in the low-dimensional settings (sample size $n \gg p$) is concerned with testing whether $\{i, j\} \in \mathcal{E}$ for all possible edges in the graph, based on some nonparametric frequency-domain test statistic such as partial coherence [10], [11], [17]–[19], [24], [25]. These approaches do not scale to high dimensions where p is comparable to sample size n . As an alternative to nonparametric modeling of time series, parametric graphical models utilizing a (Gaussian) vector autoregressive (VAR)

J.K. Tugnait is with the Department of Electrical & Computer Engineering, 200 Broun Hall, Auburn University, Auburn, AL 36849, USA. Email: tugnjak@auburn.edu .

This work was supported by the National Science Foundation under Grants CCF-1617610 and ECCS-2040536.

process model of $\mathbf{x}(t)$, have been advocated in [13], [26], [27], but these approaches are suitable for only small values of p . As an alternative to exhaustive search over various edges, a penalized maximum likelihood approach in conjunction with VAR models has been used in [14] where the penalty term incorporates sparsity constraints, making it suitable for high-dimensional setting. For every pair of series components, the corresponding partial coherence is thresholded to decide if it is zero (exclude the edge), or nonzero (include the edge). No systematic (or principled) method is given for threshold selection. Nonparametric approaches for graphical modeling of real time series in high-dimensional settings have been formulated in frequency-domain in [28], [29] using a neighborhood regression scheme, and in the form of penalized log-likelihood in frequency-domain in [30]–[32] ([32] considers latent variable graphical models). References [31], [32] exploit the framework of [30], and therefore, inherit some of its drawbacks, discussed in more detail in Sec. III-B later. [31] considers a Bayesian framework with a focus on multiple time series realizations whereas [30] deals with a single realization of the time series. Sufficient conditions for graph edge recovery are provided in [30] whereas there is no such analysis in [31], [32]. A recent approach [33] considers a vector Gaussian time series with uncorrelated samples but possibly nonstationary covariance matrices. This paper [33] addresses real-valued time series using a neighborhood regression scheme. However, the results in [33] are applied to DFT of stationary time series without analyzing the resultant complex-values series (complex in the frequency-domain), and without noting the fact the DFT over the entire observation set does not result in (approximately) uncorrelated Gaussian sequence; see Secs. II and III-B later where it is pointed out that only “half” of the DFT sequence is uncorrelated.

B. Our Contributions

As discussed in Sec. II, for “large” sample size n , the discrete Fourier transform (DFT) $\mathbf{d}_x(f_m)$, $f_m = m/n$, of real-valued $\{\mathbf{x}(t)\}_{t=0}^{n-1}$, defined in (1), is complex-valued proper Gaussian and (mutually) independent for $m = 1, 2, \dots, (n/2) - 1$ [34]. We exploit the DFT of given data to infer a sufficient statistic $\{\mathbf{d}_x(f_m)\}_{m=0}^{n/2}$ for our problem, a fact not recognized in [30] (see also Sec. III-B). This leads to a frequency-domain formulation of the graph modeling problem for based on $\{\mathbf{d}_x(f_m)\}_{m=1}^{(n/2)-1}$, neglecting $\mathbf{d}_x(f_m)$ at $m = 0$ and $m = n/2$ where the DFT is real-valued Gaussian. The objective then is to estimate the inverse PSD of the data via optimization of a sparse-group lasso-based penalized log-likelihood cost function that is formulated in the frequency-domain. This part is similar to [30] with two major differences: (i) we use sufficient statistic $\{\mathbf{d}_x(f_m)\}_{m=1}^{n/2-1}$ whereas [30] uses PSD estimates for normalized frequencies in $[0, 1]$, appealing to Whittle approximation [35], [36], (ii) we use a sparse-group lasso penalty on off-diagonal elements of inverse PSD estimates at individual frequencies (lasso) as well as jointly across all frequencies (group lasso), whereas [30] uses only a group lasso penalty that is applied to all elements, including diagonal elements, of inverse PSD estimates. Once

the inverse PSD is estimated, the CIG is then inferred from the estimated inverse PSD.

We propose an alternating direction method of multipliers (ADMM) approach for optimization of the sparse-group lasso-based penalized log-likelihood formulation of the problem. Note that [30] also used ADMM but for group lasso formulation. We provide sufficient conditions for convergence in the Frobenius norm of the inverse PSD estimators to the true value, jointly across all frequencies, where the number of frequencies are allowed to increase with sample size. This results also yields a rate of convergence. [30] provides sufficient conditions for consistent graph edge recovery when the number of frequencies are fixed independent of sample size, and [31], [32] offer no theoretical analysis. We also empirically investigate selection of the tuning parameters needed for our sparse-group lasso approach, based on Bayesian information criterion (BIC). No such results are available in [30].

We present numerical results for both synthetic and real data to illustrate the proposed approach. In synthetic data example the ground truth is known and this allows for assessment of the efficacy of various approaches. In real data example where the ground truth is unknown, our goal is visualization and exploration of the dependency structure underlying the data. In both cases we wish to compare our proposed approach with the widely used i.i.d. modeling approach where the underlying time series is either assumed to be i.i.d., or one uses only the covariance of the data.

Preliminary versions of parts of this paper appear in conference papers [37], [38]. The sufficient statistic for our problem was first discussed in [37] where a sparse-group lasso problem was also formulated in frequency-domain. But an alternating minimization (AM) based solution to this problem, using the penalty method, is given in [37]. The performance of this method depends upon the penalty parameter, and strictly speaking, convergence of this solution to the desired solution requires the penalty parameter to become large, which can make the problem numerically ill-conditioned. Use of the ADDM approach mitigates the dependence on the penalty parameter used in the AM approach. The theoretical analysis (Theorem 1) presented in Sec. V is partially given in [38] where the proof is incomplete. In this paper we provide a complete proof and also correct some typos. In turn, the proof of Theorem 1 relies on some prior results in [39] which deal with complex-valued Gaussian vectors, not time series. Lemma 1 appears in [37] without a proof. Lemma 3 is from [38] where a complete proof is given, here we simply state and use it. A version of Lemma 4 is stated without proof in [39], here we give a complete proof. Lots of details of proof of Theorem 1 are missing in [38]. The material in Secs. III-A5, IV and VI of this paper does not appear in [37]–[39].

C. Outline and Notation

The rest of the paper is organized as follows. The sufficient statistic in the frequency-domain for our problem and the resulting sparse-group lasso-based penalized log-likelihood formulation of the problem are presented in Sec. II. An ADMM algorithm is presented in Sec. III to optimize the

objective function to estimate the inverse PSD and the edges in the graph. Selection of the tuning parameters based on BIC is presented in Sec. IV. In Sec. V we analyze consistency (Theorem 1) of the proposed approach. Numerical results based on synthetic as well as real data are presented in Sec. VI to illustrate the proposed approach. Proofs of Lemma 1 and Theorem 1 are given in Appendices A and A, respectively.

Given $\mathbf{A} \in \mathbb{C}^{p \times p}$, we use $\phi_{\min}(\mathbf{A})$, $\phi_{\max}(\mathbf{A})$, $|\mathbf{A}|$, $\text{tr}(\mathbf{A})$ and $\text{etr}(\mathbf{A})$ to denote the minimum eigenvalue, maximum eigenvalue, determinant, trace, and exponential of trace of \mathbf{A} , respectively. The Kronecker product of matrices \mathbf{A} and \mathbf{B} is denoted by $\mathbf{A} \otimes \mathbf{B}$. For $\mathbf{B} \in \mathbb{C}^{p \times q}$, we define $\|\mathbf{B}\| = \sqrt{\phi_{\max}(\mathbf{B}^H \mathbf{B})}$, $\|\mathbf{B}\|_F = \sqrt{\text{tr}(\mathbf{B}^H \mathbf{B})}$ and $\|\mathbf{B}\|_1 = \sum_{i,j} |B_{ij}|$ where B_{ij} is the (i,j) -th element of \mathbf{B} , also denoted by $[\mathbf{B}]_{ij}$. Given $\mathbf{A} \in \mathbb{C}^{p \times p}$, $\mathbf{A}^+ = \text{diag}(\mathbf{A})$ is a diagonal matrix with the same diagonal as \mathbf{A} , and $\mathbf{A}^- = \mathbf{A} - \mathbf{A}^+$ is \mathbf{A} with all its diagonal elements set to zero. We use \mathbf{A}^{-*} for $(\mathbf{A}^*)^{-1}$, the inverse of complex conjugate of \mathbf{A} , and $\mathbf{A}^{-\top}$ for $(\mathbf{A}^\top)^{-1}$. The notation $\mathbf{y}_n \sim \mathcal{O}_P(\mathbf{x}_n)$ for random $\mathbf{y}_n, \mathbf{x}_n \in \mathbb{C}^p$ means that for any $\varepsilon > 0$, there exists $0 < M < \infty$ such that $P(\|\mathbf{y}_n\| \leq M\|\mathbf{x}_n\|) \geq 1 - \varepsilon \forall n \geq 1$. The notation $\mathbf{x} \sim \mathcal{N}_c(\mathbf{m}, \Sigma)$ denotes a complex random vector \mathbf{x} that is circularly symmetric, complex Gaussian with mean \mathbf{m} and covariance Σ , and $\mathbf{x} \sim \mathcal{N}_r(\mathbf{m}, \Sigma)$ denotes real-valued Gaussian \mathbf{x} with mean \mathbf{m} and covariance Σ .

II. SUFFICIENT STATISTIC AND PENALIZED LOG-LIKELIHOOD

Given $\mathbf{x}(t)$ for $t = 0, 1, 2, \dots, n-1$. Define the (normalized) DFT $\mathbf{d}_x(f_m)$ of $\mathbf{x}(t)$, ($j = \sqrt{-1}$),

$$\mathbf{d}_x(f_m) = \frac{1}{\sqrt{n}} \sum_{t=0}^{n-1} \mathbf{x}(t) \exp(-j2\pi f_m t) \quad (1)$$

where

$$f_m = m/n, \quad m = 0, 1, \dots, n-1. \quad (2)$$

Since $\{\mathbf{x}(t)\}$ is Gaussian, so is $\mathbf{d}_x(f_m)$. Note that $\mathbf{d}_x(f_m)$ is periodic in m with period n , and is periodic in normalized frequency f_m with period 1. Since $\mathbf{x}(t)$ is real-valued, we have $\mathbf{d}_x^*(f_m) = \mathbf{d}_x(-f_m) = \mathbf{d}_x(1 - f_m)$, so $\mathbf{d}_x(f_m)$ for $m = 0, 1, \dots, (n/2)$, (n even), completely determines $\mathbf{d}_x(f_m)$ for all integers m . As proved in [40, p. 280, Sec. 6.2], for any statistical inference problem, the complete sample is a sufficient statistic, and so is any one-to-one function of a sufficient statistic. Since the inverse DFT yields (one-to-one transformation) $\mathbf{x}(t) = \frac{1}{\sqrt{n}} \sum_{m=0}^{n-1} \mathbf{d}_x(f_m) e^{j2\pi f_m t}$, the set $\{\mathbf{d}_x(f_m)\}_{m=0}^{n-1}$ is a sufficient statistic, which can be further reduced to $\{\mathbf{d}_x(f_m)\}_{m=0}^{n/2}$ since $\mathbf{x}(t)$ is real-valued, inducing symmetries $\mathbf{d}_x^*(f_m) = \mathbf{d}_x(-f_m) = \mathbf{d}_x(1 - f_m)$. Thus, the set of complex-valued random vectors $\{\mathbf{d}_x(f_m)\}_{m=0}^{n/2}$ is a sufficient statistic for our problem.

We need the following assumption in order to invoke [34, Theorem 4.4.1], used extensively later.

(A1) The p -dimensional time series $\{\mathbf{x}(t)\}_{t=-\infty}^{\infty}$ is zero-mean stationary and Gaussian, satisfying

$$\sum_{\tau=-\infty}^{\infty} |[\mathbf{R}_{xx}(\tau)]_{k\ell}| < \infty \text{ for every } k, \ell \in V.$$

It follows from [34, Theorem 4.4.1] that under assumption (A1), asymptotically (as $n \rightarrow \infty$), $\mathbf{d}_x(f_m)$, $m = 1, 2, \dots, (n/2) - 1$, (n even), are independent proper (i.e., circularly symmetric), complex Gaussian $\mathcal{N}_c(\mathbf{0}, \mathbf{S}_x(f_m))$ random vectors, respectively. Also, asymptotically, $\mathbf{d}_x(f_0)$ and $\mathbf{d}_x(f_{n/2})$, (n even), are independent real Gaussian $\mathcal{N}_r(\mathbf{0}, \mathbf{S}_x(f_0))$ and $\mathcal{N}_r(\mathbf{0}, \mathbf{S}_x(f_{n/2}))$ random vectors, respectively, independent of $\mathbf{d}_x(f_m)$, $m \in [1, (n/2) - 1]$. We will ignore these two frequency points f_0 and $f_{n/2}$. Suppose $\mathbf{S}_x(f_m)$ is locally smooth (a standard assumption in PSD estimation), so that $\mathbf{S}_x(f_m)$ is (approximately) constant over $K = 2m_t + 1$ consecutive frequency points f_m 's. Pick

$$\tilde{f}_k = \frac{(k-1)K + m_t + 1}{N}, \quad k = 1, 2, \dots, M, \quad (3)$$

$$M = \left\lfloor \frac{\frac{N}{2} - m_t - 1}{K} \right\rfloor, \quad (4)$$

yielding M equally spaced frequencies \tilde{f}_k in the interval $(0, 0.5)$. By local smoothness

$$\mathbf{S}_x(\tilde{f}_{k,\ell}) = \mathbf{S}_x(\tilde{f}_k) \text{ for } \ell = -m_t, -m_t + 1, \dots, m_t, \quad (5)$$

where

$$\tilde{f}_{k,\ell} = \frac{(k-1)K + m_t + 1 + \ell}{n}. \quad (6)$$

Then the joint probability density function (pdf) of the sufficient statistic, for large n , is

$$f_{\mathbf{D}}(\mathbf{D}) = \prod_{k=1}^M \frac{e^{-\text{tr}(\tilde{\mathbf{D}}(\tilde{f}_k) \mathbf{S}_x^{-1}(\tilde{f}_k))}}{\pi^{Kp} |\mathbf{S}_x(\tilde{f}_k)|^K} = \prod_{k=1}^M f_{\tilde{\mathbf{D}}(\tilde{f}_k)}(\tilde{\mathbf{D}}(\tilde{f}_k)) \quad (7)$$

where

$$\tilde{\mathbf{D}}(\tilde{f}_k) = \left[\mathbf{d}_x(\tilde{f}_{k,-m_t}) \mathbf{d}_x(\tilde{f}_{k,-m_t+1}) \cdots \mathbf{d}_x(\tilde{f}_{k,m_t}) \right]^H \quad (8)$$

$$\hat{\mathbf{S}}_k = \frac{1}{K} \underbrace{\sum_{\ell=-m_t}^{m_t} \mathbf{d}_x(\tilde{f}_{k,\ell}) \mathbf{d}_x^H(\tilde{f}_{k,\ell})}_{=:\tilde{\mathbf{D}}(\tilde{f}_k)} \quad (9)$$

and $\hat{\mathbf{S}}_k$ represents PSD estimator at frequency \tilde{f}_k using unweighted frequency-domain smoothing.

In the high-dimensional case of $K < p^2$ (number of real unknowns in $\mathbf{S}_x^{-1}(\tilde{f}_k)$), one may need to use penalty terms to enforce sparsity and to make the problem well-conditioned. We wish to estimate inverse PSD matrix $\Phi_k := \mathbf{S}_x^{-1}(\tilde{f}_k)$. In terms of Φ_k we rewrite (7) as

$$\begin{aligned} f_{\tilde{\mathbf{D}}(\tilde{f}_k)}(\tilde{\mathbf{D}}(\tilde{f}_k)) &= \frac{|\Phi_k|^K \text{etr}(-K \hat{\mathbf{S}}_k \Phi_k)}{\pi^{Kp}} \\ &= \frac{|\Phi_k|^{K/2} |\Phi_k^*|^{K/2}}{\pi^{Kp}} \text{etr} \left(-\frac{K}{2} (\hat{\mathbf{S}}_k \Phi_k + \hat{\mathbf{S}}_k^* \Phi_k^*) \right) \end{aligned} \quad (10)$$

where the last expression in (10) follows by specifying the pdf of $\tilde{\mathbf{D}}$ in terms of joint pdf of $\tilde{\mathbf{D}}$ and $\tilde{\mathbf{D}}^*$ (correct way to handle complex variates [41]). Then we have the log-likelihood (up to some constants) [37]

$$\ln f_{\mathbf{D}}(\mathbf{D}) \propto -G(\{\Phi\}, \{\Phi^*\}) \quad (11)$$

$$:= \sum_{k=1}^M \frac{1}{2} \left[(\ln |\Phi_k| + \ln |\Phi_k^*|) - \text{tr} \left(\hat{\mathbf{S}}_k \Phi_k + \hat{\mathbf{S}}_k^* \Phi_k^* \right) \right]. \quad (12)$$

Imposing a sparse-group sparsity constraint [4], [42]–[44], minimize a penalized version of negative log-likelihood w.r.t. $\{\Phi\} = \{\Phi_k, k = 1, 2, \dots, M\}$

$$L_{SGL}(\{\Phi\}) = G(\{\Phi\}, \{\Phi^*\}) + P(\{\Phi\}), \quad (13)$$

$$P(\{\Phi\}) = \bar{\lambda}_1 \sum_{k=1}^M \sum_{i \neq j}^p \left| [\Phi_k]_{ij} \right| + \bar{\lambda}_2 \sum_{i \neq j}^p \|\Phi^{(ij)}\| \quad (14)$$

$$\text{where } \Phi^{(ij)} := [[\Phi_1]_{ij} \ [\Phi_2]_{ij} \ \dots \ [\Phi_M]_{ij}]^\top \in \mathbb{C}^M \quad (15)$$

and $\bar{\lambda}_1, \bar{\lambda}_2 \geq 0$ are tuning parameters. We will set $\bar{\lambda}_1 = \alpha\lambda$ and $\bar{\lambda}_2 = (1 - \alpha)\lambda$ with $\lambda > 0$, and $\alpha \in [0, 1]$ providing a convex combination of lasso and group-lasso penalties [42], [43]. Parameter $\lambda > 0$ is a penalty (tuning) parameter used to control sparsity, and $0 \leq \alpha \leq 1$ yields a convex combination of lasso and group lasso penalties ($\alpha = 0$ gives the group-lasso fit while $\alpha = 1$ yields the lasso fit). In (14), an ℓ_1 penalty term is applied to each off-diagonal element of Φ_k via $\alpha\lambda \left| [\Phi_k]_{ij} \right|$ (lasso), and to the off-block-diagonal group of M terms via $(1 - \alpha)\lambda \sqrt{\sum_{k=1}^M \left| [\Phi_k]_{ij} \right|^2}$ (group lasso).

Remark 1. We have complex-valued Φ_k 's. So we use Wirtinger calculus (complex differential calculus) [41, Appendix 2], [45] coupled with corresponding definition of sub-differential/subgradients [46], [47], to analyze and minimize strictly convex $L_{SGL}(\{\Phi\})$ w.r.t. complex $\{\Phi\}$ using the necessary and sufficient KKT conditions for a global optimum. Consider a complex-valued $z = \mathbf{x} + j\mathbf{y} \in \mathbb{C}^p$, \mathbf{x}, \mathbf{y} reals, and a real-valued scalar function $g(z) = g(z, z^*) = g(\mathbf{x}, \mathbf{y})$. In Wirtinger calculus, one views $g(z, z^*)$ as a function of two independent vectors z and z^* , instead of a function a single z , and defines

$$\frac{\partial g(z, z^*)}{\partial z^*} := \frac{1}{2} \left[\frac{\partial g}{\partial \mathbf{x}} + j \frac{\partial g}{\partial \mathbf{y}} \right] \quad (16)$$

$$\frac{\partial g(z, z^*)}{\partial z} := \frac{1}{2} \left[\frac{\partial g}{\partial \mathbf{x}} - j \frac{\partial g}{\partial \mathbf{y}} \right]; \quad (17)$$

see [41, Appendix 2]. For $g(z)$ one defines its subdifferential $\partial g(z_0)$ at a point z_0 as [46], [47]

$$\partial g(z_0) = \left\{ \mathbf{s} \in \mathbb{C}^p : g(z) \geq g(z_0) + 2 \operatorname{Re}(\mathbf{s}^H (z - z_0)) \text{ for all } z \in \mathbb{C}^p \right\}. \quad (18)$$

In particular, for scalar $z \in \mathbb{C}$, $g(z) = |z|$, we have [47]

$$\partial |z| = t = \begin{cases} z/|z| & \text{if } z \neq 0 \\ \{v : |v| \leq 1, v \in \mathbb{C}\} & \text{if } z = 0 \end{cases}. \quad (19)$$

Similarly, with $h_k(x) := g(z_1, z_2, \dots, z_{k-1}, x, z_{k+1}, \dots, z_p)$, $x \in \mathbb{C}$, the partial subdifferential $\partial g_{z_0k}(z) := \partial h_k(z_0k)$ is the subdifferential $\partial h_k(z_0k)$ of $h_k(x)$ at z_0k . Also [47]

$$\partial g(z_0) = \left. \frac{\partial g(z)}{\partial z^*} \right|_{z=z_0} \quad (20)$$

when this partial derivative exists and g is convex. \square

III. OPTIMIZATION VIA ADMM

To optimize $L_{SGL}(\{\Phi\})$, using variable splitting, one may reformulate as in [37]:

$$\min_{\{\Phi\}, \{\mathbf{W}\}} \left\{ G(\{\Phi\}, \{\Phi^*\}) + P(\{\mathbf{W}\}) \right\} \quad (21)$$

subject to $\mathbf{W}_k = \Phi_k \succ \mathbf{0}$, $k = 1, 2, \dots, M$, where $\{\Phi\} = \{\Phi_k, k = 1, 2, \dots, M\}$ and $\{\mathbf{W}\} = \{\mathbf{W}_k, k = 1, 2, \dots, M\}$.

In ADMM, we consider the scaled augmented Lagrangian for this problem [46], [48]

$$L_\rho(\{\Phi\}, \{\mathbf{W}\}, \{\mathbf{U}\}) = G(\{\Phi\}, \{\Phi^*\}) + P(\{\mathbf{W}\}) + \frac{\rho}{2} \sum_{k=1}^M \|\Phi_k - \mathbf{W}_k + \mathbf{U}_k\|_F^2 \quad (22)$$

where $\{\mathbf{U}\} = \{\mathbf{U}_k, k = 1, 2, \dots, M\}$ are dual variables, and $\rho > 0$ is the ‘‘penalty parameter’’ [48].

A. ADMM Algorithm

Given the results $\{\Phi^{(m)}\}, \{\mathbf{W}^{(m)}\}, \{\mathbf{U}^{(m)}\}$ of the m th iteration, in the $(m + 1)$ st iteration, an ADMM algorithm executes the following three updates:

- $\{\Phi^{(m+1)}\} \leftarrow \arg \min_{\{\Phi\}} L_\rho(\{\Phi\}, \{\mathbf{W}^{(m)}\}, \{\mathbf{U}^{(m)}\})$
- $\{\mathbf{W}^{(m+1)}\} \leftarrow \arg \min_{\{\mathbf{W}\}} L_\rho(\{\Phi^{(m+1)}\}, \{\mathbf{W}\}, \{\mathbf{U}^{(m)}\})$
- $\{\mathbf{U}^{(m+1)}\} \leftarrow \{\mathbf{U}^{(m)}\} + (\{\Phi^{(m+1)}\} - \{\mathbf{W}^{(m+1)}\})$

1) *Update (a):* Notice that $L_\rho(\{\Phi\}, \{\mathbf{W}^{(m)}\}, \{\mathbf{U}^{(m)}\})$ is separable in k with $L_\rho(\{\Phi\}, \{\mathbf{W}^{(m)}\}, \{\mathbf{U}^{(m)}\}) = \sum_{k=1}^M \frac{1}{2} L_{\rho k}(\Phi_k, \mathbf{W}_k^{(m)}, \mathbf{U}_k^{(m)})$ up to some terms not dependent upon Φ_k 's, where

$$L_{\rho k}(\Phi_k, \mathbf{W}_k^{(m)}, \mathbf{U}_k^{(m)}) := \ln |\Phi_k| + \ln |\Phi_k^*| - \operatorname{tr}(\hat{\mathbf{S}}_k \Phi_k + \hat{\mathbf{S}}_k^* \Phi_k^*) + \rho \|\Phi_k - \mathbf{W}_k^{(m)} + \mathbf{U}_k^{(m)}\|_F^2. \quad (23)$$

As in [48, Sec. 6.5] but accounting for complex-valued vectors/matrices in this paper compared to real-valued vectors/matrices in [4], and therefore using the Wirtinger calculus, the solution to $\arg \min_{\Phi_k} L_{\rho k}(\Phi_k, \mathbf{W}_k^{(m)}, \mathbf{U}_k^{(m)})$ is as follows. A necessary and sufficient condition for a global optimum is that the gradient of $L_{\rho k}(\Phi_k, \mathbf{W}_k^{(m)}, \mathbf{U}_k^{(m)})$ w.r.t. Φ_k^* , given by (25), vanishes, with $\Phi_k = \hat{\Phi}_k^H \succ \mathbf{0}$ (we set $\mathbf{A} = \mathbf{W}_k^{(m)} - \mathbf{U}_k^{(m)}$):

$$\mathbf{0} = \frac{\partial L_{\rho k}(\Phi_k, \mathbf{W}_k^{(m)}, \mathbf{U}_k^{(m)})}{\partial \Phi_k^*} = -(\Phi_k^H)^{-1} + \hat{\mathbf{S}}_k^H + \rho(\Phi_k - \mathbf{A}) \quad (24)$$

$$= \hat{\mathbf{S}}_k - \Phi_k^{-1} + \rho(\Phi_k - \mathbf{A}). \quad (25)$$

The solution to (25) follows as for the real-valued case discussed in [48, Sec. 6.5]. Rewrite (25) as

$$\hat{\mathbf{S}}_k - \rho \mathbf{A} = \hat{\mathbf{S}}_k - \rho(\mathbf{W}_k^{(m)} - \mathbf{U}_k^{(m)}) = \Phi_k^{-1} - \rho \Phi_k. \quad (26)$$

Let $\mathbf{V} \mathbf{D} \mathbf{V}^H$ denote the eigen-decomposition of the Hermitian matrix $\hat{\mathbf{S}}_k - \rho \mathbf{A}$ where \mathbf{D} is diagonal with real values on the diagonal, and $\mathbf{V} \mathbf{V}^H = \mathbf{V}^H \mathbf{V} = \mathbf{I}$. Then we have

$$\mathbf{D} = \mathbf{V}^H (\Phi_k^{-1} - \rho \Phi_k) \mathbf{V} = \tilde{\mathbf{D}}^{-1} - \rho \tilde{\mathbf{D}} \quad (27)$$

where $\tilde{\mathbf{D}} := \mathbf{V}^H \Phi_k \mathbf{V}$. Assume that $\tilde{\mathbf{D}}$ is a diagonal matrix and solve (27) for diagonal $\tilde{D}_{\ell\ell}$. That is, $\tilde{D}_{\ell\ell}$ should satisfy

$$D_{\ell\ell} = 1/\tilde{D}_{\ell\ell} - \rho\tilde{D}_{\ell\ell}. \quad (28)$$

The solution

$$\tilde{D}_{\ell\ell} = \frac{1}{2\rho} \left(-D_{\ell\ell} + \sqrt{|D_{\ell\ell}|^2 + 4\rho} \right) \quad (29)$$

satisfies (28) and yields $\tilde{D}_{\ell\ell} > 0$ for any $\rho > 0$. Therefore, so constructed $\tilde{\mathbf{D}} \succ 0$, and hence, $\Phi_k = \Phi_k^{(m+1)} = \mathbf{V} \tilde{\mathbf{D}} \mathbf{V}^H \succ 0$ satisfies (25) and (26).

2) *Update (b)*: Update $\{\mathbf{W}_k^{(m+1)}\}_{k=1}^M$ as the minimizer w.r.t. $\{\mathbf{W}\}_{k=1}^M$ of

$$\frac{\rho}{2} \sum_{k=1}^M \|\mathbf{W}_k - (\Phi_k^{(m+1)} + \mathbf{U}_k^{(m)})\|_F^2 + P(\{\mathbf{W}\}). \quad (30)$$

Here we use Lemma 1 first stated (but not proved) in [37], and is based on the real-valued results of [43]. Lemma 1 is proved in Appendix A.

Lemma 1. Given $\mathbf{a} \in \mathbb{C}^q$, $\lambda_i > 0$ ($i = 1, 2$), $h(\boldsymbol{\theta}) = (1/2)\|\mathbf{a} - \boldsymbol{\theta}\|^2 + \lambda_1 \sum_{i=1}^q |\theta_i| + \lambda_2 \|\boldsymbol{\theta}\|$ is minimized w.r.t. $\boldsymbol{\theta} \in \mathbb{C}^q$ by $\hat{\boldsymbol{\theta}}$ with the i th component

$$\hat{\theta}_i = \left(1 - \frac{\lambda_2}{\|\mathbf{S}(\mathbf{a}, \lambda_1)\|} \right)_+ S(a_i, \lambda_1) \quad (31)$$

where $(b)_+ := \max(0, b)$, soft-thresholding operator $S(b, \beta) := (1 - \beta/|b|)_+ b$ (for complex scalar $b \neq 0$), and vector operator $[\mathbf{S}(\mathbf{a}, \beta)]_j = S(a_j, \beta)$, $a_j = [\mathbf{a}]_j$. •

Define $\mathbf{A}_k = \Phi_k^{(m+1)} + \mathbf{U}_k^{(m)}$. Invoking Lemma 1, the solution to minimization of (30) is

$$[\mathbf{W}_k^{(m+1)}]_{ij} = \begin{cases} [\mathbf{A}_k]_{ii}, & \text{if } i = j \\ S([\mathbf{A}_k]_{ij}, \frac{\alpha\lambda}{\rho}) \left(1 - \frac{(1-\alpha)\lambda}{\rho\|\mathbf{S}(\mathbf{A}_k^{(ij)}, \alpha\lambda/\rho)\|} \right)_+ & \text{if } i \neq j \end{cases}$$

3) *Update (c)*: For the scaled Lagrangian formulation of ADMM [48], for $k = 1, 2, \dots, M$, update $\mathbf{U}_k^{(m+1)} = \mathbf{U}_k^{(m)} + (\Phi_k^{(m+1)} - \mathbf{W}_k^{(m+1)})$.

4) *Algorithm Outline*:

- (i) Initialize the variables: $\Phi_k^{(0)} = \mathbf{I}_p$, $\mathbf{W}_k^{(0)} = \mathbf{U}_k^{(0)} = \mathbf{0}$ for $k = 1, 2, \dots, M$. Pick scalar $\rho > 0$.
- (ii) Until convergence, for $m = 1, 2, \dots$, do steps (iii)-(v):
- (iii) For $k = 1, \dots, M$, update $\Phi_k^{(m+1)}$ as in Sec. III-A1.
- (iv) For $k = 1, \dots, M$, update $\mathbf{W}_k^{(m+1)}$ as in Sec. III-A2
- (v) For $k = 1, \dots, M$, update $\mathbf{U}_k^{(m+1)}$ as in Sec. III-A3.
- (vi) Denote the converged estimates as $\hat{\Phi}_k$, $k = 1, \dots, M$. Edge selection:

$$\text{If } \|\hat{\Phi}^{(ij)}\| > 0, \text{ then } \{i, j\} \in \mathcal{E}, \text{ else } \{i, j\} \notin \mathcal{E}. \quad (32)$$

5) *Stopping Rule, Variable Penalty ρ , and Convergence*:

We use the stopping (convergence) criterion following [48, Sec. 3.3.1] and varying penalty parameter $\rho^{(m)}$ at the m th iteration, following [48, Sec. 3.4.1]. The stopping criterion is based on primal and dual residuals being small where, in our

case, at $(m+1)$ st iteration, the primal residual is given by the vectorized matrix

$$\mathbf{R}_p = \left[\Phi_1^{(m+1)} - \mathbf{W}_1^{(m+1)}, \dots, \Phi_M^{(m+1)} - \mathbf{W}_M^{(m+1)} \right]$$

and the dual residual by the vectorized matrix

$$\mathbf{R}_d = \rho^{(m)} \left[\mathbf{W}_1^{(m+1)} - \mathbf{W}_1^{(m)}, \dots, \mathbf{W}_M^{(m+1)} - \mathbf{W}_M^{(m)} \right].$$

The convergence criterion is met when the norms of these residuals are below primary and dual tolerances τ_{pri} and τ_{dual} , respectively, where τ_{pri} and τ_{dual} are chosen using an absolute and relative criterion based on user chosen absolute and relative tolerances τ_{abs} and τ_{rel} [48, Sec. 3.3.1]. Let

$$\begin{aligned} e_1 &= \|\Phi_1^{(m+1)}, \dots, \Phi_M^{(m+1)}\|_F, \\ e_2 &= \|\mathbf{W}_1^{(m+1)}, \dots, \mathbf{W}_M^{(m+1)}\|_F, \\ e_3 &= \|\mathbf{U}_1^{(m+1)}, \dots, \mathbf{U}_M^{(m+1)}\|_F. \end{aligned}$$

Then

$$\begin{aligned} \tau_{pri} &= p\sqrt{M} \tau_{abs} + \tau_{rel} \max(e_1, e_2) \\ \tau_{dual} &= p\sqrt{M} \tau_{abs} + \tau_{rel} e_3 / \rho^{(m)}. \end{aligned}$$

The convergence criterion is: $d_p := \|\mathbf{R}_p\|_F \leq \tau_{pri}$ and $d_d := \rho^{(m)} \|\mathbf{R}_d\|_F \leq \tau_{dual}$.

As stated in [48, Sec. 3.4.1], one may use ‘‘possibly different penalty parameters $\rho^{(m)}$ for each iteration, with the goal of improving the convergence in practice, as well as making performance less dependent on the initial choice of the penalty parameter.’’ For scaled Lagrangian formulation, the variable penalty ρ is updated as [48, Sec. 3.4.1]

$$\rho^{(m+1)} = \begin{cases} 2\rho^{(m)} & \text{if } d_p > \mu d_d \\ \rho^{(m)}/2 & \text{if } d_d > \mu d_p \\ \rho^{(m)} & \text{otherwise} \end{cases}$$

for some $\mu > 1$. For all numerical results presented later, we used $\rho_0 = 2$, $\mu = 10$, and $\tau_{abs} = \tau_{rel} = 10^{-4}$.

The objective function $L_{SGL}(\{\Phi\})$, given by (13), is strictly convex in $\{\Phi\}$ for $\Phi_k \succ \mathbf{0}$, $k = 1, 2, \dots, M$. It is also closed, proper and lower semi-continuous. Hence, for any fixed $\rho > 0$, the ADMM algorithm is guaranteed to converge [48, Sec. 3.2], in the sense that we have primal residual convergence to 0, dual residual convergence to 0, and objective function convergence to the optimal value. For varying ρ , the convergence of ADMM has not yet been proven [48, Sec. 3.4.1].

B. Comparison with Existing Works

As noted earlier, $\{\mathbf{d}_x(f_m)\}_{m=0}^{n/2}$ is a sufficient statistic for this problem. However, in [30] (and [31], [32]), one uses some estimate of PSD $\mathcal{S}_x(f_m)$, or $\mathbf{d}_x(f_m)$, for $m = 0, 1, \dots, n-1$ appealing to Whittle approximation [35], [36]. Also, in [30], frequencies (f_m or f_k in our notation) are fixed a priori as $(f-1)/F \in [0, 1)$, $f = 1, 2, \dots, F$, for some even integer F . For instance, in the simulation example of [30], $F = 4$, leading to four frequencies $\{0, 0.25, 0.5, 0.75\}$ for any data size n . Note that $\mathcal{S}_x(0.75) = \mathcal{S}_x^*(0.25)$, so there is no new information in it. Also, $\mathcal{S}_x(0)$ and $\mathcal{S}_x(0.5)$ are real-valued, not

complex. Furthermore [30] considers the penalty term $P(\{\Phi\})$ with $\lambda_1 = 0$ and the summation in the second term also includes terms for $i = j$ (i.e., the diagonal terms which are always nonzero).

IV. BIC FOR TUNING PARAMETER SELECTION

Let $\hat{\Phi}_k$, $k = 1, \dots, M$, denote the converged estimates, as noted in item (vi) of Sec. III-A4. Given n and choice of K and M , the Bayesian information criterion (BIC) is given by

$$\begin{aligned} \text{BIC}(\lambda, \alpha) = & 2K \sum_{k=1}^M \left(-\ln |\hat{\Phi}_k| + \text{tr} \left(\hat{S}_k \hat{\Phi}_k \right) \right) \\ & + \ln(2KM) \sum_{k=1}^M (\# \text{ of nonzero elements in } \hat{\Phi}_k) \end{aligned} \quad (33)$$

where $2KM$ are total number of real-valued measurements in frequency-domain and $2K$ are number of real-valued measurements per frequency point, with total M frequencies in $(0, \pi)$. Each nonzero off-diagonal element of $\hat{\Phi}_k$ consists of two real variables, but since $\hat{\Phi}_k$ is Hermitian, the number of (nonzero) real unknowns in $\hat{\Phi}_k$ equal the number of nonzero elements of $\hat{\Phi}_k$. Pick α and λ to minimize BIC. We use BIC to first select λ over a grid of values with fixed α , and then with selected λ , we search over α values in $[0, 0.3]$. This sequential search is computationally less demanding than a two-dimensional search.

We search over λ in the range $[\lambda_\ell, \lambda_u]$ selected via the following heuristic (as in [44]). For $\alpha = \alpha_0 (=0.1)$, we first find the smallest λ , labeled λ_{sm} , for which we get a no-edge model (i.e., $|\hat{\mathcal{E}}| = 0$). Then we set $\lambda_u = \lambda_{sm}/2$ and $\lambda_\ell = \lambda_u/10$. The given choice of λ_u precludes “extremely” sparse models while that of λ_ℓ precludes “very” dense models. The choice $\alpha \in [0, 0.3]$ reflects the fact that group-lasso penalty across all frequencies is more important ((i, j) th element of inverse PSD at all frequencies must be zero for edge $\{i, j\} \notin \mathcal{E}$) than lasso penalty at individual frequencies.

V. CONSISTENCY

Define $p \times (pM)$ matrix Ω :

$$\Omega = [\Phi_1 \ \Phi_2 \ \dots \ \Phi_M]. \quad (34)$$

With $0 \leq \alpha \leq 1$, re-express the objective function (13) as

$$\begin{aligned} L_{SGL}(\Omega) = & G(\{\Phi\}, \{\Phi^*\}) + \alpha \lambda_n \sum_{k=1}^{M_n} \sum_{\substack{i,j=1 \\ i \neq j}}^{p_n} |[\Phi_k]_{ij}| \\ & + (1 - \alpha) \lambda_n \sum_{\substack{i,j=1 \\ i \neq j}}^{p_n} \sqrt{\sum_{k=1}^{M_n} |[\Phi_k]_{ij}|^2} \end{aligned} \quad (35)$$

where we now allow p , M , K (see (3)), and λ to be functions of sample size n , denoted as p_n , M_n , K_n and λ_n , respectively. Note that $K_n M_n \approx n/2$. Pick $K_n = a_1 n^\gamma$ and $M_n = a_2 n^{1-\gamma}$ for some $0.5 < \gamma < 1$ so that $M_n/K_n \rightarrow 0$ as $n \rightarrow \infty$.

We follow proof technique of [22] which deals with i.i.d time series models and lasso penalty, to establish our main result, Theorem 1. Assume

(A2) Define the true edge set of the graph by \mathcal{E}_0 , implying that $\mathcal{E}_0 = \{\{i, j\} : [\mathcal{S}_0^{-1}(f)]_{ij} \neq 0, i \neq j, 0 \leq f \leq 0.5\}$ where $\mathcal{S}_0(f)$ denotes the true PSD of $\mathbf{x}(t)$. (We also use Φ_{0k} for $\mathcal{S}_0^{-1}(\tilde{f}_k)$ where \tilde{f}_k is as in (3), and use Ω_0 to denote the true value of Ω). Assume that $\text{card}(\mathcal{E}_0) = |\mathcal{E}_0| \leq s_{n0}$.

(A3) The minimum and maximum eigenvalues of $p_n \times p_n$ PSD $\mathcal{S}_0(f) \succ \mathbf{0}$ satisfy

$$\begin{aligned} 0 < \beta_{\min} & \leq \min_{f \in [0, 0.5]} \phi_{\min}(\mathcal{S}_0(f)) \\ & \leq \max_{f \in [0, 0.5]} \phi_{\max}(\mathcal{S}_0(f)) \leq \beta_{\max} < \infty. \end{aligned}$$

Here β_{\min} and β_{\max} are not functions of n (or p_n).

Let $\hat{\Omega}_\lambda = \arg \min_{\Omega: \Phi_k \succ \mathbf{0}} L_{SGL}(\Omega)$. Theorem 1 whose proof is given in Appendix A, establishes consistency of $\hat{\Omega}_\lambda$. *Theorem 1 (Consistency)*. For $\tau > 2$, let

$$C_0 = 80 \max_{\ell, f} ([\mathcal{S}_0(f)]_{\ell\ell}) \sqrt{\frac{2 \ln(16 p_n^\tau M_n)}{\ln(p_n)}}. \quad (36)$$

Given any real numbers $\delta_1 \in (0, 1)$, $\delta_2 > 0$ and $C_1 > 0$, let

$$R = C_2 C_0 / \beta_{\min}^2, \quad C_2 = 2(2 + C_1 + \delta_2)(1 + \delta_1)^2, \quad (37)$$

$$r_n = \sqrt{\frac{M_n(p_n + s_{n0}) \ln(p_n)}{K_n}}, \quad C_2 r_n = o(1), \quad (38)$$

$$N_1 = 2 \ln(16 p_n^\tau M_n), \quad (39)$$

$$N_2 = \arg \min \left\{ n : r_n \leq \frac{\delta_1 \beta_{\min}}{C_2 C_0} \right\}. \quad (40)$$

Suppose the regularization parameter λ_n and $\alpha \in [0, 1]$ satisfy

$$\begin{aligned} C_0 \sqrt{\frac{\ln(p_n)}{K_n}} & \leq \frac{\lambda_n}{\sqrt{M_n}} \\ & \leq \frac{C_1 C_0}{1 + \alpha(\sqrt{M_n} - 1)} \sqrt{\left(1 + \frac{p_n}{s_{n0}}\right) \frac{\ln(p_n)}{K_n}}. \end{aligned} \quad (41)$$

Then if the sample size is such that $n > \max\{N_1, N_2\}$ and assumptions (A1)-(A3) hold true, $\hat{\Omega}_\lambda$ satisfies

$$\|\hat{\Omega}_\lambda - \Omega_0\|_F \leq R r_n \quad (42)$$

with probability greater than $1 - 1/p_n^{\tau-2}$. A sufficient condition for the lower bound in (41) to be less than the upper bound for every $\alpha \in [0, 1]$ is $C_1 = 2(1 + \alpha(\sqrt{M_n} - 1))$. In terms of rate of convergence, $\|\hat{\Omega}_\lambda - \Omega_0\|_F = \mathcal{O}_P(C_1 r_n)$ •

Remark 2. If $\alpha = 0$, then C_1 is a constant, and therefore, $\|\hat{\Omega}_\lambda - \Omega_0\|_F = \mathcal{O}_P(r_n)$. If $\alpha > 0$, then $C_1 = \mathcal{O}(\sqrt{M_n})$, therefore, $\|\hat{\Omega}_\lambda - \Omega_0\|_F = \mathcal{O}_P(\sqrt{M_n} r_n)$. As noted before, since $K_n M_n \approx n/2$, if one picks $K_n = a_1 n^\gamma$ and $M_n = a_2 n^{1-\gamma}$ for some $0 < \gamma < 1$, then we must have $\frac{2}{3} < \gamma < 1$ so that $M_n^2/K_n \rightarrow 0$ as $n \rightarrow \infty$, ensuring $C_2 r_n = o(1)$. Therefore, for $\alpha > 0$, one needs $\sqrt{\frac{M_n^2(p_n + s_{n0}) \ln(p_n)}{K_n}} \rightarrow 0$ so that $\|\hat{\Omega}_\lambda - \Omega_0\|_F = \mathcal{O}_P(\sqrt{M_n} r_n) \rightarrow 0$ as $n \rightarrow \infty$. □

VI. NUMERICAL EXAMPLES

We now present numerical results for both synthetic and real data to illustrate the proposed approach. In synthetic data example the ground truth is known and this allows for assessment of the efficacy of various approaches. In real data example where the ground truth is unknown, our goal is visualization and exploration of the dependency structure underlying the data.

A. Synthetic Data

Consider $p = 128$, 16 clusters (communities) of 8 nodes each, where nodes within a community are not connected to any nodes in other communities. Within any community of 8 nodes, the data are generated using a vector autoregressive (VAR) model of order 3. Consider community q , $q = 1, 2, \dots, 16$. Then $\mathbf{x}^{(q)}(t) \in \mathbb{R}^8$ is generated as

$$\mathbf{x}^{(q)}(t) = \sum_{i=1}^3 \mathbf{A}_i^{(q)} \mathbf{x}^{(q)}(t-i) + \mathbf{w}^{(q)}(t)$$

Only 10% of entries of $\mathbf{A}_i^{(q)}$'s are nonzero and the nonzero elements are independently and uniformly distributed over $[-0.8, 0.8]$. We then check if the VAR(3) model is stable with all eigenvalues of the companion matrix ≤ 0.95 in magnitude; if not, we re-draw randomly till this condition is fulfilled. The overall data $\mathbf{x}(t)$ is given by $\mathbf{x}(t) = [\mathbf{x}^{(1)\top}(t) \dots \mathbf{x}^{(16)\top}(t)]^\top \in \mathbb{R}^p$ with $\mathbf{w}^{(q)}(t)$ as i.i.d. zero-mean Gaussian with identity covariance matrix. First 100 samples are discarded to eliminate transients. This set-up leads to approximately 3.5% connected edges. In each run, we calculated the true PSD $\mathcal{S}(f)$ for $f \in [0, 0.5]$ at intervals of 0.01, and then take $\{i, j\} \in \mathcal{E}$ if $\sum_f |S_{ij}(f)| > 10^{-6}$.

Simulation results are shown in Fig. 1 where the performance measure is F_1 -score for efficacy in edge detection. The F_1 -score is defined as $F_1 = 2 \times \text{precision} \times \text{recall} / (\text{precision} + \text{recall})$ where $\text{precision} = |\hat{\mathcal{E}} \cap \mathcal{E}_0| / |\hat{\mathcal{E}}|$, $\text{recall} = |\hat{\mathcal{E}} \cap \mathcal{E}_0| / |\mathcal{E}_0|$, and \mathcal{E}_0 and $\hat{\mathcal{E}}$ denote the true and estimated edge sets, respectively. For our proposed approach, we consider three different values of $M \in \{2, 4, 6\}$ for five samples sizes $n \in \{128, 256, 512, 1024, 2048\}$. For $M = 2$, we used $K = 31, 63, 127, 255, 511$ for $n = 128, 256, 512, 1024, 2048$, respectively, for $M = 4$, we used $K = 15, 31, 63, 127, 255$ for $n = 128, 256, 512, 1024, 2048$, respectively, and for $M = 6$, we used $K = 9, 21, 41, 85, 169$ for $n = 128, 256, 512, 1024, 2048$, respectively. These approaches are labeled as “proposed: M=2,” “proposed: M=4,” and “proposed: M=6,” in Fig. 1. The tuning parameters λ and α were selected by searching over a grid of values to maximize the F_1 -score (over 100 runs). The search for α was confined to $[0, 0.3]$. For a fixed $\alpha = 0.1$, we first picked the best λ value, and then with fixed best λ value, search over $\alpha \in [0, 0.3]$. Fig. 1 shows the results for thus optimized (λ, α) . In practice, one cannot calculate the F_1 -score since ground truth is unknown. For $M = 4$ we selected (λ, α) in each run via BIC as discussed in Sec. IV (where knowledge of the ground truth is not needed). The obtained results based on 50 runs are shown in Fig. 1, labeled as “proposed: M=4,BIC.” The conventional i.i.d. modeling approach exploits only the

sample covariance $\frac{1}{n} \sum_{t=0}^{n-1} \mathbf{x}(t) \mathbf{x}^\top(t)$ whereas the proposed approaches exploit the entire correlation function (equivalently PSD), and thus, can deliver better performance. In Fig. 1, the label “IID model” stands for the ADMM lasso approach ([48, Sec. 6.4]) that models data as i.i.d., and the corresponding results are based on 100 runs with lasso parameter λ selected by exhaustive search over a grid of values to maximize F_1 score. We also show the results of the ADMM approach of [30], labeled “GMS” (graphical model selection), which was applied with $F = 4$ (four frequency points, corresponds to our $M = 4$) and all other default settings of [30] to compute the PSDs (see also Sec. III-B). The lasso parameter λ for [30] was selected by exhaustive search over a grid of values to maximize F_1 score.

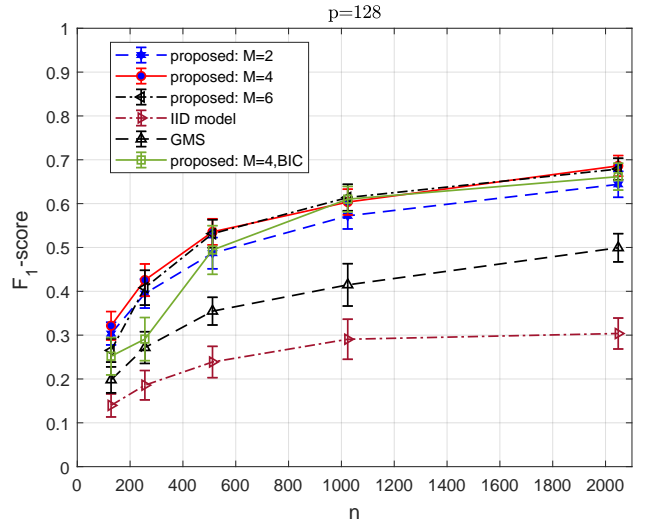


Fig. 1: F_1 -score for synthetic data example. The label “GMS” refers to the approach of [30].

It is seen from Fig. 1 that our proposed approach for all three values of M (number of normalized frequency points in $(0, 0.5)$) significantly outperforms the conventional IID model approach. The BIC-based approach for $M = 4$ yields performance that is close to that based on optimized parameter selection for $n \geq 512$. It is also seen that [30] performs better than IID modeling but much worse than our proposed sparse group lasso approach.

The conventional i.i.d. modeling approach estimates the (sparse) precision matrix $\mathbf{\Omega} = (E\{\mathbf{x}(t) \mathbf{x}^\top(t)\})^{-1}$: there is an edge $\{i, j\}$ in CIG iff $\Omega_{ij} \neq 0$. For a typical Monte Carlo run with $n = 1024$, we show the estimated weighted adjacency matrices resulting from the conventional “IID model” approach and from the “proposed: M=4,BIC” approach in Figs. 2 and 3 respectively. For the IID model approach, tuning parameter λ used is the one used for Fig. 1, selected by exhaustive search to maximize the F_1 score. Fig. 2 shows true and estimated $|\Omega_{ij}|$ as edge weights, whereas Fig. 3 shows true $\sqrt{\sum_{k=1}^M |[\Phi_k]_{ij}|^2}$ and estimated $\sqrt{\sum_{k=1}^M |[\hat{\Phi}_k]_{ij}|^2}$ as edge

weights.

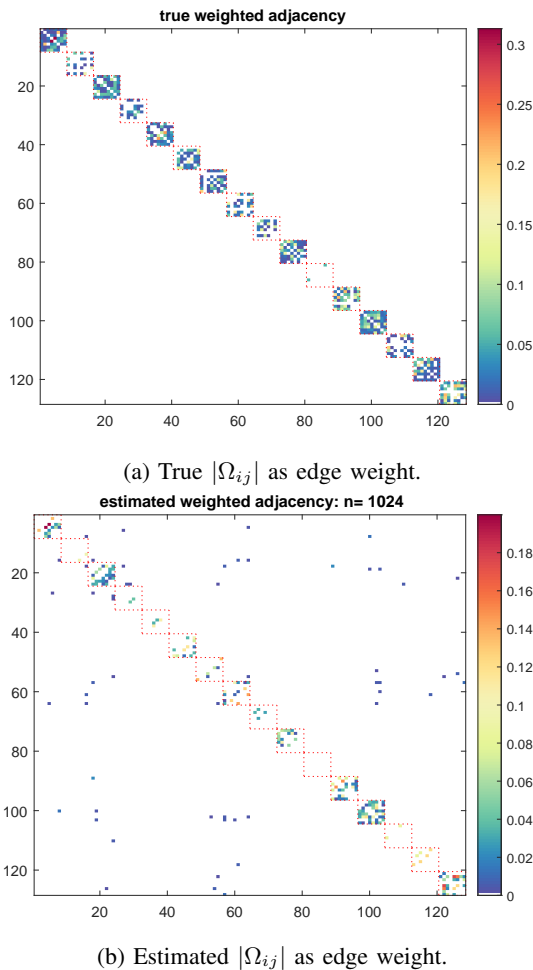


Fig. 2: IID modeling-based weighted adjacency matrices. The red squares (in dotted lines) show the communities – they are not part of the adjacency matrices.

B. Real data: Financial Time Series

We consider daily share prices (at close of the day) of 97 stocks in S&P 100 index from Jan. 1, 2013 through Jan. 1, 2018, yielding 1259 samples. This data was gathered from Yahoo Finance website. If $y_m(t)$ is share price of m th stock on day t , we consider (as is conventional in such studies [12]) $x_m(t) = \ln(y_m(t)/y_m(t-1))$ as the time series to analyze, yielding $n = 1258$ and $p = 97$. These 97 stocks are classified into 11 sectors (according to the Global Industry Classification Standard (GICS)), and we order the nodes to group them as information technology (nodes 1-12), health care (13-27), financials (28-44), real estate (45-46), consumer discretionary (47-56), industrials (57-68), communication services (69-76), consumer staples (77-87), energy (88-92), materials (93), utilities (94-97). The weighted adjacency matrices resulting from the conventional i.i.d. modeling approach and the proposed approach with $M = 4$, ($K = 155$), are shown in Fig. 4. In both cases we used BIC to determine the tuning parameters with selected $\lambda = 0.0387$ for the IID model and $(\lambda, \alpha) = (0.7, 0.3)$ for the proposed approach. While the ground truth is unknown, the dependent time series based proposed approach yields

sparser CIG (429 edges for the proposed approach versus 1293 edges for conventional modeling) which also conforms better with the GICS sector classification.

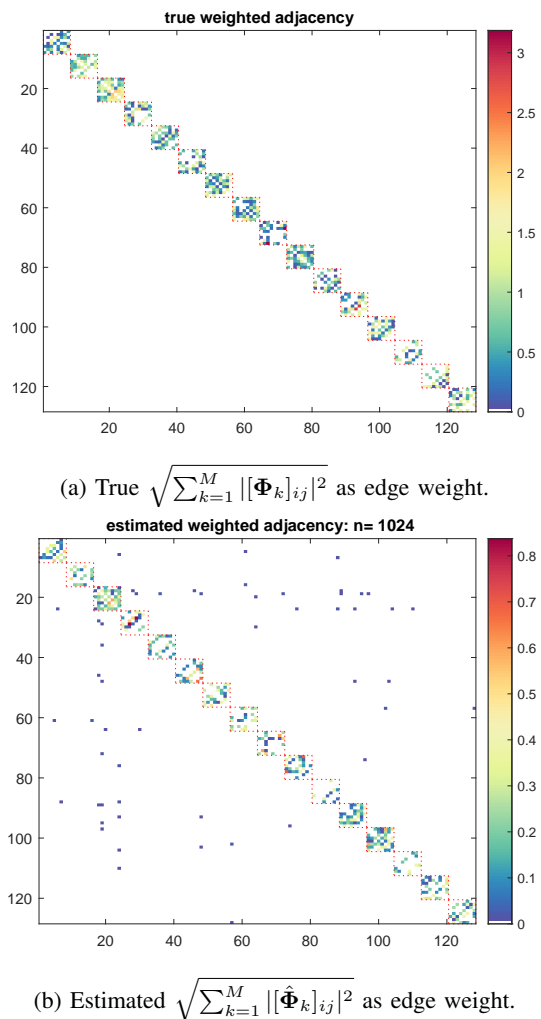


Fig. 3: Weighted adjacency matrices for dependent time series modeling: $M = 4$. The red squares (in dotted lines) show the communities – they are not part of the adjacency matrices.

VII. CONCLUSIONS

Graphical modeling of dependent Gaussian time series was considered. A sparse-group lasso-based frequency-domain formulation of the problem was proposed and analyzed where the objective was to estimate the inverse PSD of the data via optimization of a sparse-group lasso penalized log-likelihood cost function. The graphical model is then inferred from the estimated inverse PSD. We investigated an ADMM approach for optimization. We established sufficient conditions for convergence in the Frobenius norm of the inverse PSD estimators to the true value, jointly across all frequencies, where the number of frequencies were allowed to increase with sample size. We also empirically investigated selection of the tuning parameters based on Bayesian information criterion, and illustrated our approach using numerical examples utilizing both synthetic and real data. The synthetic data results show that for graph edge detection, the proposed approach significantly

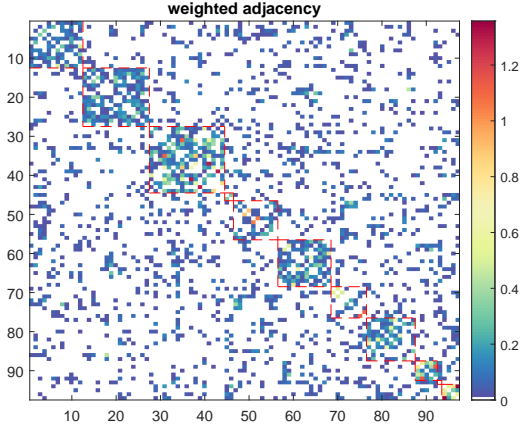
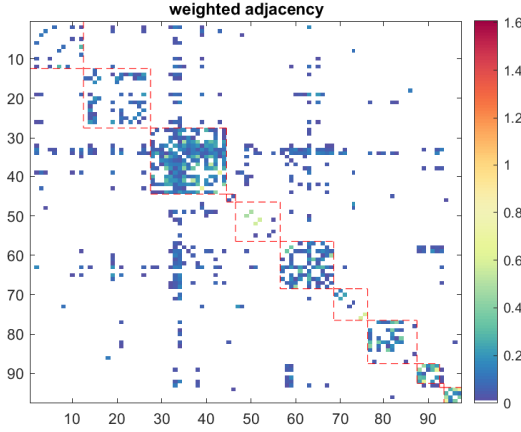
(a) Estimated $|\Omega_{i,j}|$ as edge weight; 1293 edges.(b) Estimated $\sqrt{\sum_{k=1}^M |\hat{\Phi}_k]_{ij}|^2}$ as edge weight; 429 edges.

Fig. 4: Weighted adjacency matrices for financial time series, $p = 97$, $n = 1258$. (a) IID model approach, (b) Proposed approach, $M = 4$. The red squares (in dashed lines) show the 11 GISC sectors – they are not part of the adjacency matrices.

outperformed the widely used i.i.d. modeling approach where the underlying time series is either assumed to be i.i.d., or one uses only the covariance of the data. The proposed approach also outperformed the approach of [30] for synthetic data.

APPENDIX

Lemma 1 is proved following [43] (which deals with real variables), and using Wirtinger calculus and complex subgradients. Since $h(\theta)$ is convex in θ , a necessary and sufficient condition for a global minimum at $\hat{\theta}$ is that the subdifferential of $h(\theta)$ at $\hat{\theta}$, $\partial h(\hat{\theta})$ given by (43), must contain $\mathbf{0}$:

$$\mathbf{0} \in \partial h(\hat{\theta}) = \frac{1}{2}(\hat{\theta} - \mathbf{a}) + \frac{\lambda_1}{2}\mathbf{t} + \frac{\lambda_2}{2}\mathbf{w} \quad (43)$$

where $(t_j = [t]_j, j$ th component of $\mathbf{t})$

$$\mathbf{w} = \begin{cases} \hat{\theta}/\|\hat{\theta}\| & \text{if } \hat{\theta} \neq \mathbf{0} \\ \in \{\mathbf{u} : \|\mathbf{u}\| \leq 1, \mathbf{u} \in \mathbb{C}^q\} & \text{if } \hat{\theta} = \mathbf{0} \end{cases}, \quad (44)$$

$$t_j = \begin{cases} \hat{\theta}_j/|\hat{\theta}_j| & \text{if } \hat{\theta}_j \neq 0 \\ \in \{v : |v| \leq 1, v \in \mathbb{C}\} & \text{if } \hat{\theta}_j = 0 \end{cases}. \quad (45)$$

Lemma 1 is a consequence of KKT conditions (43). We will show that (31) satisfies (43). Consider the following two cases:

- (i) Suppose $\|\mathbf{S}(\mathbf{a}, \lambda_1)\| \leq \lambda_2$. Then (31) implies that $\hat{\theta}_i = 0 \forall i$. We need to show that this solution satisfies (43), that is, given \mathbf{a} , there exist \mathbf{w} and \mathbf{t} satisfying

$$w_j = \frac{a_j - \lambda_1 t_j}{\lambda_2}, \quad j = 1, 2, \dots, q. \quad (46)$$

Following real-valued results of [43], consider minimization of $J(\mathbf{t})$, defined below, w.r.t. t_j 's subject to $|t_j|^2 \leq 1$, $j = 1, 2, \dots, q$:

$$J(\mathbf{t}) = \sum_{j=1}^q |w_j|^2 = \frac{1}{\lambda_2^2} \sum_{j=1}^q |a_j - \lambda_1 t_j|^2. \quad (47)$$

The problem is separable in t_j 's with the solution

$$\hat{t}_j = \begin{cases} a_j/\lambda_1 & \text{if } |a_j| \leq \lambda_1 \\ a_j/|a_j| & \text{if } |a_j| > \lambda_1. \end{cases} \quad (48)$$

Thus $a_j - \lambda_1 \hat{t}_j = (1 - \lambda_1/|a_j|)_+ a_j$ and with $\hat{w}_j = (a_j - \lambda_1 \hat{t}_j)/\lambda_2$, we have

$$\min_{\mathbf{t}} J(\mathbf{t}) = J(\hat{\mathbf{t}}) = \sum_{j=1}^q |\hat{w}_j|^2 = \frac{1}{\lambda_2^2} \|\mathbf{S}(\mathbf{a}, \lambda_1)\|^2 \leq 1. \quad (49)$$

Thus (43) holds for given $\hat{\mathbf{w}}$ and $\hat{\mathbf{t}}$ satisfying (44) and (45), respectively.

- (ii) Now suppose $\|\mathbf{S}(\mathbf{a}, \lambda_1)\| > \lambda_2$. Then (31) implies that $\hat{\theta} \neq \mathbf{0}$, therefore, at least one component of $\hat{\theta}$ is nonzero. Again we need to show that this solution satisfies (43). If $|a_i| \leq \lambda_1$, then $\hat{\theta}_i = 0$ and $\hat{t}_i = a_i/\lambda_1$ satisfies (45). If $|a_i| > \lambda_1$, then $\hat{\theta}_i \neq 0$ and we take $\hat{t}_i = \hat{\theta}_i/|\hat{\theta}_i|$. For an arbitrary a_i , but satisfying $\|\mathbf{S}(\mathbf{a}, \lambda_1)\| > \lambda_2$, let us express our claimed solution $\hat{\theta}_i \neq 0$ as

$$\hat{\theta}_i = \gamma \alpha_i a_i, \quad \alpha_i := (1 - \lambda_1/|a_i|)_+ \quad (50)$$

$$\gamma = 1 - \lambda_2 / \left(\sum_{j=1}^q \alpha_j^2 |a_j|^2 \right)^{1/2} > 0. \quad (51)$$

We need to show that this solution satisfies (43). The i th component of $2\partial h(\hat{\theta})$ with $\hat{\mathbf{w}}$ and $\hat{\mathbf{t}}$ satisfying (44) and (45), respectively, is

$$\begin{aligned} A &:= \hat{\theta}_i - a_i + \lambda_1 \frac{\hat{\theta}_i}{|\hat{\theta}_i|} + \lambda_2 \frac{\hat{\theta}_i}{\|\hat{\theta}\|} \\ &= \hat{\theta}_i \left[1 + \frac{\lambda_1}{|\hat{\theta}_i|} + \frac{\lambda_2}{\|\hat{\theta}\|} \right] - a_i = a_i B - a_i \end{aligned} \quad (52)$$

where, with $D := (\sum_{j=1}^q \alpha_j^2 |a_j|^2)^{1/2}$,

$$B = \gamma \alpha_i + \frac{\lambda_1}{|a_i|} + \frac{\lambda_2 \alpha_i}{D}. \quad (53)$$

The proof is completed by showing that $B = 1$. We have

$$B = \frac{\gamma \alpha_i |a_i| D + \lambda_1 D + \lambda_2 \alpha_i |a_i|}{|a_i| D} \quad (54)$$

$$= \frac{\alpha_i |a_i| D - \lambda_2 \alpha_i |a_i| + \lambda_1 D + \lambda_2 \alpha_i |a_i|}{|a_i| D} \quad (55)$$

$$= \frac{\alpha_i |a_i| + \lambda_1}{|a_i|} = \alpha_i + \frac{\lambda_1}{|a_i|} = 1 \quad (56)$$

where, for $\hat{\theta}_i \neq 0$, $\alpha_i = 1 - \lambda_1/|\alpha_i|$.

This proves the desired result \blacksquare

Our proof relies on the method of [22] which deals with i.i.d. time series models and lasso penalty, and our prior results in [39] dealing with complex Gaussian vectors (not time series). From now on we use the term ‘‘with high probability’’ (w.h.p.) to denote with probability greater than $1 - 1/p_n^{\tau-2}$. First we need several auxiliary results.

Lemma 2 below is specialization of [49, Lemma 1] to Gaussian random vectors. It follows from [49, Lemma 1] after setting the sub-Gaussian parameter σ in [49, Lemma 1] to 1. *Lemma 2.* Consider a zero-mean Gaussian random vector $\mathbf{z} \in \mathbb{R}^p$ with covariance $\mathbf{R} \succ \mathbf{0}$. Given n i.i.d. samples $\mathbf{z}(t)$, $t = 0, 1, \dots, n-1$, of \mathbf{z} , let $\hat{\mathbf{R}} = (1/n) \sum_{t=0}^{n-1} \mathbf{z}\mathbf{z}^\top$ denote the sample covariance matrix. Then $\hat{\mathbf{R}}$ satisfies the tail bound

$$P\left(\left|[\hat{\mathbf{R}} - \mathbf{R}]_{ij}\right| > \delta\right) \leq 4 \exp\left(-\frac{n\delta^2}{3200 \max_i(R_{ii}^2)}\right) \quad (57)$$

for all $\delta \in (0, 40 \max_i(R_{ii}))$ \bullet

Exploiting Lemma 2, we have Lemma 3 regarding $\hat{\mathbf{S}}_k$. We denote $\mathbf{S}_0(f_k)$ as \mathbf{S}_{0k} in this section. A proof of Lemma 3 is in [38].

Lemma 3. Under Assumption (A2), $\hat{\mathbf{S}}_k$ satisfies the tail bound

$$P\left(\max_{k,q,l} \left|[\hat{\mathbf{S}}_k - \mathbf{S}_{0k}]_{ql}\right| > C_0 \sqrt{\frac{\ln(p_n)}{K_n}}\right) \leq \frac{1}{p_n^{\tau-2}} \quad (58)$$

for $\tau > 2$, if the sample size $n > N_1$, where C_0 is defined in (36) and N_1 is defined in (39). \bullet

Lemma 4 deals with a Taylor series expansion using Wirtinger calculus.

Lemma 4. For $\Phi_k = \Phi_k^H \succ \mathbf{0}$, define a real scalar function

$$c(\Phi_k, \Phi_k^*) = \ln |\Phi_k| + \ln |\Phi_k^*|. \quad (59)$$

Let $\Phi_k = \Phi_{0k} + \Gamma_k$ with $\Phi_{0k} = \Phi_{0k}^H \succ \mathbf{0}$ and $\Gamma_k = \Gamma_k^H$. Then using Wirtinger calculus, the Taylor series expansion of $c(\Phi_k, \Phi_k^*)$ is given by

$$\begin{aligned} c(\Phi_k, \Phi_k^*) &= c(\Phi_{0k}, \Phi_{0k}^*) + \text{tr}(\Phi_{0k}^{-1} \Gamma_k + \Phi_{0k}^{-*} \Gamma_k^*) \\ &\quad - \frac{1}{2} (\text{vec}(\Gamma_k))^H (\Phi_{0k}^{-*} \otimes \Phi_{0k}^{-1}) \text{vec}(\Gamma_k) \\ &\quad - \frac{1}{2} (\text{vec}(\Gamma_k^*))^H (\Phi_{0k}^{-1} \otimes \Phi_{0k}^{-*}) \text{vec}(\Gamma_k^*) + \text{h.o.t.} \end{aligned} \quad (60)$$

where h.o.t. stands for higher-order terms in Γ_k and Γ_k^* . \bullet

Proof: Only for the proof of this lemma, we will drop the subscript k , and donate Φ_k, Φ_{0k} and Γ_k as Φ, Φ_0 and Γ , respectively. Treating Φ and Φ^* as independent variables, the Taylor series expansion of $c(\Phi, \Phi^*)$ is

$$\begin{aligned} c(\Phi, \Phi^*) &= c(\Phi_0, \Phi_0^*) + \sum_{s,t} \left(\frac{\partial c}{\partial \Phi_{0st}} \Gamma_{st} + \frac{\partial c}{\partial \Phi_{0st}^*} \Gamma_{st}^* \right) \\ &\quad + \frac{1}{2} \sum_{q,r} \sum_{s,t} [\Gamma_{qr} \quad \Gamma_{qr}^*] D_{0qrst} \begin{bmatrix} \Gamma_{st} \\ \Gamma_{st}^* \end{bmatrix} + \text{h.o.t.} \end{aligned} \quad (61)$$

where

$$\frac{\partial c}{\partial \Phi_{0st}} := \frac{\partial c(\Phi, \Phi^*)}{\partial \Phi_{st}} \Bigg|_{\substack{\Phi_{st} = \Phi_{0st} \\ \Phi_{st}^* = \Phi_{0st}^*}}, \quad (62)$$

$$\frac{\partial c}{\partial \Phi_{0st}^*} := \frac{\partial c(\Phi, \Phi^*)}{\partial \Phi_{st}^*} \Bigg|_{\substack{\Phi_{st} = \Phi_{0st} \\ \Phi_{st}^* = \Phi_{0st}^*}}, \quad (63)$$

$$\begin{aligned} D_{0qrkl} &= \begin{bmatrix} \frac{\partial^2 c(\Phi, \Phi^*)}{\partial \Phi_{qr} \partial \Phi_{st}} & \frac{\partial^2 c(\Phi, \Phi^*)}{\partial \Phi_{qr} \partial \Phi_{st}^*} \\ \frac{\partial^2 c(\Phi, \Phi^*)}{\partial \Phi_{qr}^* \partial \Phi_{st}} & \frac{\partial^2 c(\Phi, \Phi^*)}{\partial \Phi_{qr}^* \partial \Phi_{st}^*} \end{bmatrix} \Bigg|_{\substack{\Phi_{st} = \Phi_{0st}, \Phi_{st}^* = \Phi_{0st}^* \\ \Phi_{qr} = \Phi_{0qr}, \Phi_{qr}^* = \Phi_{0qr}^*}} \\ &=: \begin{bmatrix} \frac{\partial^2 c(\Phi, \Phi^*)}{\partial \Phi_{0qr} \partial \Phi_{0st}} & \frac{\partial^2 c(\Phi, \Phi^*)}{\partial \Phi_{0qr} \partial \Phi_{0st}^*} \\ \frac{\partial^2 c(\Phi, \Phi^*)}{\partial \Phi_{0qr}^* \partial \Phi_{0st}} & \frac{\partial^2 c(\Phi, \Phi^*)}{\partial \Phi_{0qr}^* \partial \Phi_{0st}^*} \end{bmatrix}. \end{aligned} \quad (64)$$

Consider the following facts [50], [51]

$$\frac{\partial \ln |\Phi|}{\partial \Phi_{st}} = [\Phi^{-\top}]_{st} = [\Phi^{-1}]_{ts} \text{ since } \frac{\partial \ln |\Phi|}{\partial \Phi} = \Phi^{-\top}, \quad (65)$$

$$\frac{\partial \ln |\Phi^*|}{\partial \Phi_{st}^*} = [\Phi^{-*}]_{ts}, \quad (66)$$

$$\frac{\partial \ln |\Phi|}{\partial \Phi_{st}^*} = 0, \quad \frac{\partial \ln |\Phi^*|}{\partial \Phi_{st}} = 0, \quad (67)$$

$$\frac{\partial^2 \ln |\Phi|}{\partial \Phi_{qr} \partial \Phi_{st}} = \frac{\partial [\Phi^{-1}]_{ts}}{\partial \Phi_{qr}} = -[\Phi^{-1}]_{tq} [\Phi^{-1}]_{rs}, \quad (68)$$

$$\frac{\partial^2 \ln |\Phi^*|}{\partial \Phi_{qr}^* \partial \Phi_{st}^*} = -[\Phi^{-*}]_{tq} [\Phi^{-*}]_{rs}, \quad (69)$$

$$\frac{\partial^2 \ln |\Phi|}{\partial \Phi_{qr} \partial \Phi_{st}^*} = \frac{\partial^2 \ln |\Phi|}{\partial \Phi_{qr}^* \partial \Phi_{st}} = \frac{\partial^2 \ln |\Phi^*|}{\partial \Phi_{qr} \partial \Phi_{st}^*} = \frac{\partial^2 \ln |\Phi^*|}{\partial \Phi_{qr}^* \partial \Phi_{st}} = 0. \quad (70)$$

Using the above partial derivatives in the first derivative terms in the Taylor series, we have

$$\begin{aligned} &\sum_{s,t} \left(\frac{\partial c}{\partial \Phi_{0st}} \Gamma_{st} + \frac{\partial c}{\partial \Phi_{0st}^*} \Gamma_{st}^* \right) \\ &= \sum_{s,t} ([\Phi_0^{-1}]_{ts} \Gamma_{st} + [\Phi_0^{-*}]_{ts} \Gamma_{st}^*) \\ &= \text{tr}(\Phi_0^{-1} \Gamma + \Phi_0^{-*} \Gamma^*). \end{aligned} \quad (71)$$

The quadratic terms in the Taylor series yield

$$\begin{aligned} &\sum_{q,r} \sum_{s,t} [\Gamma_{qr} \quad \Gamma_{qr}^*] D_{0qrst} \begin{bmatrix} \Gamma_{st} \\ \Gamma_{st}^* \end{bmatrix} \\ &= \sum_{q,r} \sum_{s,t} [\Gamma_{qr} \frac{\partial^2 c(\Phi, \Phi^*)}{\partial \Phi_{0qr} \partial \Phi_{0st}} \Gamma_{st} + \Gamma_{qr}^* \frac{\partial^2 c(\Phi, \Phi^*)}{\partial \Phi_{0qr}^* \partial \Phi_{0st}^*} \Gamma_{st}^*] \\ &= - \sum_{q,r} \sum_{s,t} \left[\Gamma_{qr} [\Phi_0^{-1}]_{tq} [\Phi_0^{-1}]_{rs} \Gamma_{st} \right. \\ &\quad \left. + \Gamma_{qr}^* [\Phi_0^{-*}]_{tq} [\Phi_0^{-*}]_{rs} \Gamma_{st}^* \right] \\ &= - \sum_{q,s} \left[\left(\sum_r \Gamma_{qr} [\Phi_0^{-1}]_{rs} \right) + \left(\sum_t \Gamma_{st} [\Phi_0^{-1}]_{tq} \right) \right] \\ &\quad - \sum_{q,s} \left[\left(\sum_r \Gamma_{qr}^* [\Phi_0^{-*}]_{rs} \right) + \left(\sum_t \Gamma_{st}^* [\Phi_0^{-*}]_{tq} \right) \right] \\ &= - \sum_{q,s} \left[[\Gamma \Phi_0^{-1}]_{qs} [\Gamma \Phi_0^{-1}]_{sq} + [\Gamma^* \Phi_0^{-*}]_{qs} [\Gamma^* \Phi_0^{-*}]_{sq} \right] \\ &= - \text{tr}(\Gamma \Phi_0^{-1} \Gamma \Phi_0^{-1} + \Gamma^* \Phi_0^{-*} \Gamma^* \Phi_0^{-*}). \end{aligned} \quad (72)$$

Given matrices \mathbf{A} and \mathbf{B} for which product \mathbf{AB} is defined, and additionally given matrix \mathbf{Y} such that product \mathbf{AYB} is defined, we have $\text{vec}(\mathbf{AYB}) = (\mathbf{B}^\top \otimes \mathbf{A})\text{vec}(\mathbf{Y})$ and $\text{tr}(\mathbf{AB}) = (\text{vec}(\mathbf{A}))^\top \text{vec}(\mathbf{B})$. Using these results we have

$$\begin{aligned} (\text{vec}(\mathbf{A}))^\top (\mathbf{D} \otimes \mathbf{B}) \text{vec}(\mathbf{C}) &= (\text{vec}(\mathbf{A}))^\top \text{vec}(\mathbf{BCD}^\top) \\ &= \text{tr}(\mathbf{A}^\top \mathbf{BCD}^\top). \end{aligned} \quad (73)$$

Using (73), we rewrite terms in (72) as

$$\begin{aligned} \text{tr}(\mathbf{\Gamma} \mathbf{\Phi}_0^{-1} \mathbf{\Gamma} \mathbf{\Phi}_0^{-1}) &= (\text{vec}(\mathbf{\Gamma}^\top))^\top (\mathbf{\Phi}_0^{-\top} \otimes \mathbf{\Phi}_0^{-1}) \text{vec}(\mathbf{\Gamma}) \\ &= (\text{vec}(\mathbf{\Gamma}))^H (\mathbf{\Phi}_0^{-*} \otimes \mathbf{\Phi}_0^{-1}) \text{vec}(\mathbf{\Gamma}), \end{aligned} \quad (74)$$

$$\text{tr}(\mathbf{\Gamma}^* \mathbf{\Phi}_0^{-*} \mathbf{\Gamma}^* \mathbf{\Phi}_0^{-*}) = (\text{vec}(\mathbf{\Gamma}^H))^\top (\mathbf{\Phi}_0^{-H} \otimes \mathbf{\Phi}_0^{-*}) \text{vec}(\mathbf{\Gamma}^*). \quad (75)$$

In (74), we have used $(\text{vec}(\mathbf{\Gamma}^\top))^\top = (\text{vec}(\mathbf{\Gamma}^*))^\top = (\text{vec}(\mathbf{\Gamma}))^H$ and $\mathbf{\Phi}_0^{-\top} = (\mathbf{\Phi}_0^\top)^{-1} = \mathbf{\Phi}_0^{-*}$, since $\mathbf{\Gamma} = \mathbf{\Gamma}^H$ and $\mathbf{\Phi}_0 = \mathbf{\Phi}_0^H$. In (75), we have used $(\text{vec}(\mathbf{\Gamma}^H))^\top = (\text{vec}(\mathbf{\Gamma}))^\top = (\text{vec}(\mathbf{\Gamma}^*))^H$ and $\mathbf{\Phi}_0^{-H} = (\mathbf{\Phi}_0^H)^{-1} = \mathbf{\Phi}_0^{-1}$. Using (71), (72), (74) and (75) in (61), we obtain the desired result (60). ■

Lemma 4 regarding Taylor series expansion immediately leads to Lemma 5 regarding Taylor series with integral remainder, needed to follow the proof of [22] pertaining to the real-valued case.

Lemma 5. With $c(\mathbf{\Phi}_k, \mathbf{\Phi}_k^*)$ and $\mathbf{\Phi}_k = \mathbf{\Phi}_{0k} + \mathbf{\Gamma}_k$ as in Lemma 4, the Taylor series expansion of $c(\mathbf{\Phi}_k, \mathbf{\Phi}_k^*)$ in integral remainder form is given by (v is real)

$$\begin{aligned} c(\mathbf{\Phi}_k, \mathbf{\Phi}_k^*) &= c(\mathbf{\Phi}_{0k}, \mathbf{\Phi}_{0k}^*) + \text{tr}(\mathbf{\Phi}_{0k}^{-1} \mathbf{\Gamma}_k + \mathbf{\Phi}_{0k}^{-*} \mathbf{\Gamma}_k^*) \\ &\quad - \mathbf{g}^H(\mathbf{\Gamma}_k) \left(\int_0^1 (1-v) \mathbf{H}(\mathbf{\Phi}_{0k}, \mathbf{\Gamma}_k, v) dv \right) \mathbf{g}(\mathbf{\Gamma}_k) \end{aligned} \quad (76)$$

where

$$\mathbf{g}(\mathbf{\Gamma}_k) = \begin{bmatrix} \text{vec}(\mathbf{\Gamma}_k) \\ \text{vec}(\mathbf{\Gamma}_k^*) \end{bmatrix}, \quad \mathbf{H}(\mathbf{\Phi}_{0k}, \mathbf{\Gamma}_k, v) = \begin{bmatrix} \mathbf{H}_{11k} & \mathbf{0} \\ \mathbf{0} & \mathbf{H}_{22k} \end{bmatrix} \quad (77)$$

$$\mathbf{H}_{11k} = (\mathbf{\Phi}_{0k} + v\mathbf{\Gamma}_k)^{-*} \otimes (\mathbf{\Phi}_{0k} + v\mathbf{\Gamma}_k)^{-1} \quad (78)$$

and

$$\mathbf{H}_{22k} = (\mathbf{\Phi}_{0k} + v\mathbf{\Gamma}_k)^{-1} \otimes (\mathbf{\Phi}_{0k} + v\mathbf{\Gamma}_k)^{-*} \quad (79)$$

We now turn to the proof of Theorem 1.

Proof of Theorem 1. Let $\mathbf{\Omega} = \mathbf{\Omega}_0 + \mathbf{\Delta}$ where

$$\mathbf{\Delta} = [\mathbf{\Gamma}_1 \ \mathbf{\Gamma}_2 \ \cdots \ \mathbf{\Gamma}_{M_n}] \quad (80)$$

$$\mathbf{\Gamma}_k = \mathbf{\Phi}_k - \mathbf{\Phi}_{0k}, \quad k = 1, 2, \dots, M_n, \quad (81)$$

and $\mathbf{\Phi}_k, \mathbf{\Phi}_{0k}$ are both Hermitian positive-definite, implying $\mathbf{\Gamma}_k = \mathbf{\Gamma}_k^H$. Let

$$Q(\mathbf{\Omega}) := \mathcal{L}_{SGL}(\mathbf{\Omega}) - \mathcal{L}_{SGL}(\mathbf{\Omega}_0). \quad (82)$$

The estimate $\hat{\mathbf{\Omega}}_\lambda$, denoted by $\hat{\mathbf{\Omega}}$ hereafter suppressing dependence upon λ , minimizes $Q(\mathbf{\Omega})$, or equivalently, $\hat{\mathbf{\Delta}} = \hat{\mathbf{\Omega}} - \mathbf{\Omega}_0$ minimizes $G(\mathbf{\Delta}) := Q(\mathbf{\Omega}_0 + \mathbf{\Delta})$. We will follow the method of proof of [22, Theorem 1] pertaining to real-valued i.i.d. time series. Consider the set

$$\Theta_n(R) := \{ \mathbf{\Delta} : \mathbf{\Gamma}_k = \mathbf{\Gamma}_k^H \ \forall k, \|\mathbf{\Delta}\|_F = Rr_n \} \quad (83)$$

where R and r_n are as in (37) and (38), respectively. Observe that $G(\mathbf{\Delta})$ is a convex function of $\mathbf{\Delta}$, and

$$G(\hat{\mathbf{\Delta}}) = Q(\mathbf{\Omega}_0 + \hat{\mathbf{\Delta}}) \leq G(\mathbf{0}) = 0. \quad (84)$$

Therefore, if we can show that

$$\inf_{\mathbf{\Delta}} \{ G(\mathbf{\Delta}) : \mathbf{\Delta} \in \Theta_n(R) \} > 0, \quad (85)$$

the minimizer $\hat{\mathbf{\Delta}}$ must be inside the sphere defined by $\Theta_n(R)$, and hence

$$\|\hat{\mathbf{\Delta}}\|_F \leq Rr_n. \quad (86)$$

Using Lemma 5 we rewrite $G(\mathbf{\Delta})$ as

$$G(\mathbf{\Delta}) = \sum_{k=1}^{M_n} \left(\frac{1}{2} A_{1k} + \frac{1}{2} A_{2k} + A_{3k} \right) + A_4, \quad (87)$$

where, noting that $\mathbf{\Phi}_{0k}^{-1} = \mathbf{S}_{0k}$,

$$A_{1k} = \mathbf{g}^H(\mathbf{\Gamma}_k) \left(\int_0^1 (1-v) \mathbf{H}(\mathbf{\Phi}_{0k}, \mathbf{\Gamma}_k, v) dv \right) \mathbf{g}(\mathbf{\Gamma}_k), \quad (88)$$

$$A_{2k} = \text{tr} \left((\hat{\mathbf{S}}_k - \mathbf{S}_{0k}) \mathbf{\Gamma}_k + (\hat{\mathbf{S}}_k - \mathbf{S}_{0k})^* \mathbf{\Gamma}_k^* \right), \quad (89)$$

$$A_{3k} = \bar{\lambda}_1 (\|\mathbf{\Phi}_{0k}^- + \mathbf{\Gamma}_k^- \|_1 - \|\mathbf{\Phi}_{0k}^- \|_1), \quad (90)$$

$$A_4 = \bar{\lambda}_2 \sum_{i \neq j}^{p_n} (\|\mathbf{\Omega}_0^{(ij)} + \mathbf{\Delta}^{(ij)}\|_F - \|\mathbf{\Omega}_0^{(ij)}\|_F), \quad (91)$$

$$\mathbf{\Omega}_0^{(ij)} := [[\mathbf{\Phi}_{01}]_{ij} \ \cdots \ [\mathbf{\Phi}_{0M_n}]_{ij}]^\top \in \mathbb{C}^{M_n}, \quad (92)$$

$$\mathbf{\Delta}^{(ij)} := [[\mathbf{\Gamma}_1]_{ij} \ \cdots \ [\mathbf{\Gamma}_{M_n}]_{ij}]^\top \in \mathbb{C}^{M_n}. \quad (93)$$

Define

$$d_{1n} := \sqrt{\frac{\ln(p_n)}{K_n}}, \quad d_{2n} := d_{1n} \sqrt{p_n + s_{n0}}. \quad (94)$$

We first bound A_{1k} 's and A_1 . Note that $\mathbf{H}(\mathbf{\Phi}_{0k}, \mathbf{\Gamma}_k, v)$ is a Hermitian matrix and its eigenvalues consist of the eigenvalues of \mathbf{H}_{11k} and \mathbf{H}_{22k} . Since the eigenvalues of $\mathbf{A} \otimes \mathbf{B}$ are the product of the eigenvalues of \mathbf{A} and eigenvalues of \mathbf{B} for Hermitian \mathbf{A} and \mathbf{B} , the eigenvalues of \mathbf{H}_{11k} are the product of the eigenvalues of $(\mathbf{\Phi}_{0k} + v\mathbf{\Gamma}_k)^{-*}$ and that of $(\mathbf{\Phi}_{0k} + v\mathbf{\Gamma}_k)^{-1}$. But these two matrices have the same set of eigenvalues since one matrix is the complex conjugate of the other, and both have real eigenvalues since they are Hermitian. Since $\mathbf{H}_{11k} = \mathbf{H}_{22k}^*$, it follows that the eigenvalues of \mathbf{H}_{11k} are the same as the eigenvalues of \mathbf{H}_{22k} . Thus

$$\begin{aligned} \phi_{\min}(\mathbf{H}(\mathbf{\Phi}_{0k}, \mathbf{\Gamma}_k, v)) &= \phi_{\min}(\mathbf{H}_{11k}) = \phi_{\min}(\mathbf{H}_{22k}) \\ &= \phi_{\min}^2((\mathbf{\Phi}_{0k} + v\mathbf{\Gamma}_k)^{-1}) = \phi_{\max}^{-2}(\mathbf{\Phi}_{0k} + v\mathbf{\Gamma}_k). \end{aligned} \quad (95)$$

Since $\mathbf{x}^H \mathbf{A} \mathbf{x} \geq \phi_{\min}(\mathbf{A}) \|\mathbf{x}\|^2$, we have

$$\begin{aligned} A_{1k} &\geq \|\mathbf{g}(\mathbf{\Gamma}_k)\|^2 \phi_{\min} \left(\int_0^1 (1-v) \mathbf{H}(\mathbf{\Phi}_{0k}, \mathbf{\Gamma}_k, v) dv \right) \\ &\geq 2 \|\text{vec}(\mathbf{\Gamma}_k)\|^2 \int_0^1 (1-v) dv \min_{0 \leq v \leq 1} \phi_{\min}(\mathbf{H}(\mathbf{\Phi}_{0k}, \mathbf{\Gamma}_k, v)) \\ &= \|\mathbf{\Gamma}_k\|_F^2 \min_{0 \leq v \leq 1} \phi_{\max}^{-2}(\mathbf{\Phi}_{0k} + v\mathbf{\Gamma}_k), \end{aligned} \quad (96)$$

where we have used the facts that $\int_0^1 (1-v) dv = 1/2$. Since

$$\phi_{\max}(\Phi_{0k} + v\Gamma_k) \leq \|\Phi_{0k} + v\Gamma_k\| \leq \|\Phi_{0k}\| + v\|\Gamma_k\|, \quad (97)$$

we have

$$\begin{aligned} \phi_{\max}^{-2}(\Phi_{0k} + v\Gamma_k) &\geq (\|\Phi_{0k}\| + v\|\Gamma_k\|)^{-2} \\ &\geq (\|\Phi_{0k}\| + \|\Gamma_k\|)^{-2} \text{ for } 0 \leq v \leq 1. \end{aligned} \quad (98)$$

Thus,

$$A_{1k} \geq \frac{\|\Gamma_k\|_F^2}{(\|\Phi_{0k}\| + \|\Gamma_k\|)^2} \geq \|\Gamma_k\|_F^2 (\beta_{\min}^{-1} + Rr_n)^{-2} \quad (99)$$

where we have used the fact that $\|\Phi_{0k}\| = \|\mathbf{S}_{0k}^{-1}\| = \phi_{\max}(\mathbf{S}_{0k}^{-1}) = (\phi_{\min}(\mathbf{S}_{0k}))^{-1} \leq \beta_{\min}^{-1}$ and $\|\Gamma_k\| \leq \|\Gamma_k\|_F \leq \|\Delta\|_F = Rr_n = \mathcal{O}(r_n)$. Therefore,

$$2A_1 := \sum_{k=1}^{M_n} A_{1k} \geq \frac{\sum_{k=1}^{M_n} \|\Gamma_k\|_F^2}{(\beta_{\min}^{-1} + Rr_n)^2} = \frac{\|\Delta\|_F^2}{(\beta_{\min}^{-1} + Rr_n)^2} \quad (100)$$

Turning to A_{2k} , we have

$$|A_{2k}| \leq 2L_{21k} + 2L_{22k} \quad (101)$$

where

$$L_{21k} = \left| \sum_{\substack{i,j \\ i \neq j}} [\hat{\mathbf{S}}_k - \mathbf{S}_{0k}]_{ij} \Gamma_{kji} \right| = \left| \sum_{\substack{i,j \\ i \neq j}} [\hat{\mathbf{S}}_k - \mathbf{S}_{0k}]_{ij}^* \Gamma_{kji}^* \right|, \quad (102)$$

$$L_{22k} = \left| \sum_i [\hat{\mathbf{S}}_k - \mathbf{S}_{0k}]_{ii} \Gamma_{kii} \right| = \left| \sum_i [\hat{\mathbf{S}}_k - \mathbf{S}_{0k}]_{ii}^* \Gamma_{kii}^* \right|. \quad (103)$$

To bound L_{21k} , using Lemma 3, with probability $> 1 - 1/p_n^{\tau-2}$,

$$L_{21k} \leq \|\Gamma_k^-\|_1 \max_{i,j} |[\hat{\mathbf{S}}_k - \hat{\mathbf{S}}_{0k}]_{ij}| \leq \|\Gamma_k^-\|_1 C_0 d_{1n}. \quad (104)$$

Using Cauchy-Schwartz inequality and Lemma 3, with probability $> 1 - 1/p_n^{\tau-2}$,

$$\begin{aligned} L_{22k} &\leq \|\Gamma_k^+\|_F \sqrt{\sum_{i=1}^{p_n} |[\hat{\mathbf{S}}_k - \hat{\mathbf{S}}_{0k}]_{ii}|^2} \\ &\leq \|\Gamma_k^+\|_F \sqrt{p_n} \max_{1 \leq i \leq p_n} |[\hat{\mathbf{S}}_k - \hat{\mathbf{S}}_{0k}]_{ii}| \\ &\leq \|\Gamma_k^+\|_F \sqrt{p_n} C_0 d_{1n} \\ &\leq \|\Gamma_k^+\|_F C_0 d_{2n} \end{aligned} \quad (105)$$

where s_{n0} is the cardinality of the true edge set \mathcal{E}_0 (see Assumption (A1)). Thus, with probability $> 1 - 1/p_n^{\tau-2}$,

$$|A_{2k}| \leq 2C_0 (\|\Gamma_k^-\|_1 d_{1n} + \|\Gamma_k^+\|_F d_{2n}). \quad (106)$$

Hence with $A_2 = \sum_{k=1}^{M_n} (1/2) A_{2k}$,

$$|A_2| \leq \sum_{k=1}^{M_n} (1/2) |A_{2k}| \leq C_0 \sum_{k=1}^{M_n} (d_{1n} \|\Gamma_k^-\|_1 + d_{2n} \|\Gamma_k^+\|_F). \quad (107)$$

We now derive an alternative bound on A_2 . We have w.h.p.

$$|A_2| \leq \sum_{i,j=1}^{p_n} \sum_{k=1}^{M_n} |[(\hat{\mathbf{S}} - \mathbf{S}_{0k})_{ij}] \cdot |[\Gamma_k]_{ij}| \quad (108)$$

$$\leq C_0 d_{1n} \sum_{i,j=1}^{p_n} \sum_{k=1}^{M_n} |[\Gamma_k]_{ij}| \quad (109)$$

$$\leq C_0 d_{1n} \sum_{i,j=1}^{p_n} (\sqrt{M_n} \|\Delta^{(ij)}\|_F) \quad (110)$$

$$= \sqrt{M_n} C_0 d_{1n} (\|\tilde{\Delta}^-\|_1 + \|\tilde{\Delta}^+\|_1) \quad (111)$$

where $\tilde{\Delta} \in \mathbb{R}^{p_n \times p_n}$ has its (i, j) th element $\tilde{\Delta}_{ij} = \|\Delta^{(ij)}\|_F$.

We now bound A_{3k} . Let \mathcal{E}_0^c denote the complement of \mathcal{E}_0 , given by $\mathcal{E}_0^c = \{\{i, j\} : [\mathbf{S}_0^{-1}(f)]_{ij} \equiv 0, i \neq j, 0 \leq f \leq 0.5\}$. For an index set \mathcal{B} and a matrix $\mathbf{C} \in \mathbb{C}^{p \times p}$, we write $\mathbf{C}_{\mathcal{B}}$ to denote a matrix in $\mathbb{C}^{p \times p}$ such that $[\mathbf{C}_{\mathcal{B}}]_{ij} = C_{ij}$ if $(i, j) \in \mathcal{B}$, and $[\mathbf{C}_{\mathcal{B}}]_{ij} = 0$ if $(i, j) \notin \mathcal{B}$. Then $\Gamma_k^- = \Gamma_{k\mathcal{E}_0}^- + \Gamma_{k\mathcal{E}_0^c}^-$, and $\|\Gamma_k^-\|_1 = \|\Gamma_{k\mathcal{E}_0}^-\|_1 + \|\Gamma_{k\mathcal{E}_0^c}^-\|_1$. We have

$$\begin{aligned} A_{3k} &= \bar{\lambda}_1 (\|\Phi_{0k}^- + \Gamma_k^-\|_1 - \|\Phi_{0k}^-\|_1) \\ &= \bar{\lambda}_1 (\|\Phi_{0k}^- + \Gamma_{k\mathcal{E}_0}^-\|_1 + \|\Gamma_{k\mathcal{E}_0^c}^-\|_1 - \|\Phi_{0k}^-\|_1) \\ &\geq \bar{\lambda}_1 (\|\Gamma_{k\mathcal{E}_0^c}^-\|_1 - \|\Gamma_{k\mathcal{E}_0}^-\|_1) \end{aligned} \quad (112)$$

leading to $(A_3 = \sum_{k=1}^{M_n} A_{3k})$

$$A_3 \geq \bar{\lambda}_1 \sum_{k=1}^{M_n} (\|\Gamma_{k\mathcal{E}_0^c}^-\|_1 - \|\Gamma_{k\mathcal{E}_0}^-\|_1). \quad (113)$$

Similarly,

$$A_4 \geq \bar{\lambda}_2 (\|\tilde{\Delta}_{\mathcal{E}_0^c}^-\|_1 - \|\tilde{\Delta}_{\mathcal{E}_0}^-\|_1). \quad (114)$$

By Cauchy-Schwartz inequality, $\|\Gamma_{k\mathcal{E}_0}^-\|_1 \leq \sqrt{s_{n0}} \|\Gamma_{k\mathcal{E}_0}^-\|_F \leq \sqrt{s_{n0}} \|\Gamma_k\|_F$, hence

$$\sum_{k=1}^{M_n} \|\Gamma_{k\mathcal{E}_0}^-\|_1 \leq \sqrt{M_n s_{n0}} \|\Delta\|_F. \quad (115)$$

Set $\|\Gamma_k^-\|_1 = \|\Gamma_{k\mathcal{E}_0}^-\|_1 + \|\Gamma_{k\mathcal{E}_0^c}^-\|_1$ in A_2 of (107) to deduce that w.h.p.

$$\begin{aligned} \alpha A_2 + A_3 &\geq \alpha (\lambda_n - C_0 d_{1n}) \sum_{k=1}^{M_n} \|\Gamma_{k\mathcal{E}_0^c}^-\|_1 \\ &\quad - \alpha (C_0 d_{1n} + \lambda_n) \sum_{k=1}^{M_n} \|\Gamma_{k\mathcal{E}_0}^-\|_1 - \alpha C_0 d_{2n} \sum_{k=1}^{M_n} \|\Gamma_k^+\|_F \\ &\geq -\alpha \left((C_0 d_{1n} + \lambda_n) \sqrt{s_{n0}} - C_0 d_{2n} \right) \sqrt{M_n} \|\Delta\|_F \end{aligned} \quad (116)$$

where we have used the fact that $\lambda_n \geq C_0 \sqrt{M_n} d_{1n} \geq C_0 d_{1n}$ and $\sum_{k=1}^{M_n} \|\Gamma_k^+\|_F \leq \sqrt{M_n} \|\Delta\|_F$. Now use A_2 of (111) to deduce that w.h.p.

$$\begin{aligned} (1 - \alpha) A_2 + A_4 &\geq (1 - \alpha) \left((\lambda_n - C_0 \sqrt{M_n} d_{1n}) \|\tilde{\Delta}_{\mathcal{E}_0^c}^-\|_1 \right. \\ &\quad \left. - (C_0 \sqrt{M_n} d_{1n} + \lambda_n) \|\tilde{\Delta}_{\mathcal{E}_0}^-\|_1 - C_0 \sqrt{M_n p_n} d_{1n} \|\Delta\|_F \right) \\ &\geq -(1 - \alpha) \|\Delta\|_F \left(\lambda_n \sqrt{s_{n0}} + C_0 \sqrt{M_n} d_{1n} (\sqrt{s_{n0}} + \sqrt{p_n}) \right) \end{aligned} \quad (117)$$

where we have used the facts that $\lambda_n \geq C_0 \sqrt{M_n} d_{1n}$, and $\|\tilde{\Delta}_{\mathcal{E}_0}^-\|_1 \leq \sqrt{s_{n0}} \|\tilde{\Delta}_{\mathcal{E}_0}^-\|_F \leq \sqrt{s_{n0}} \|\Delta\|_F$ (by Cauchy-Schwartz inequality).

Since $r_n = \sqrt{M_n} d_{2n} > \sqrt{M_n s_{n0}} d_{1n}$, w.h.p. we have

$$\begin{aligned} A_2 + A_3 + A_4 &\geq -\|\Delta\|_F \left(\alpha(2C_0 r_n + \lambda_n \sqrt{M_n s_{n0}}) \right. \\ &\quad \left. + (1 - \alpha)(\lambda_n \sqrt{s_{n0}} + 2C_0 r_n) \right) \\ &\geq -\|\Delta\|_F \left(2C_0 r_n + \lambda_n \sqrt{s_{n0}} (\alpha \sqrt{M_n} + (1 - \alpha)) \right) \\ &\geq -\|\Delta\|_F \left((2 + C_1) C_0 r_n \right) \end{aligned} \quad (118)$$

where we have used the fact that, by (38) and (41), $\lambda_n \sqrt{s_{n0}} (\alpha \sqrt{M_n} + (1 - \alpha)) \leq C_1 C_0 r_n$. Using (87), (100) and (118), and $\|\Delta\|_F = R r_n$, we have w.h.p.

$$G(\Delta) \geq \|\Delta\|_F^2 \left[\frac{1}{2} (\beta_{\min}^{-1} + R r_n)^{-2} - \frac{(2 + C_1) C_0}{R} \right]. \quad (119)$$

For $n \geq N_2$, if we pick R as specified in (37), we obtain $R r_n \leq R r_{N_2} \leq \delta_1 / \beta_{\min}$. Then

$$\begin{aligned} \frac{1}{(\beta_{\min}^{-1} + R r_n)^2} &\geq \frac{\beta_{\min}^2}{(1 + \delta_1)^2} = \frac{2(2 + C_1 + \delta_2) C_0}{R} \\ &> \frac{2(2 + C_1) C_0}{R}, \end{aligned}$$

implying $G(\Delta) > 0$ w.h.p. This proves the desired result. ■

REFERENCES

- [1] J. Whittaker, *Graphical Models in Applied Multivariate Statistics*. New York: Wiley, 1990.
- [2] S.L. Lauritzen, *Graphical models*. Oxford, UK: Oxford Univ. Press, 1996.
- [3] P. Bühlmann and S. van de Geer, *Statistics for High-Dimensional data*. Berlin: Springer, 2011.
- [4] P. Danaher, P. Wang and D.M. Witten, "The joint graphical lasso for inverse covariance estimation across multiple classes," *J. Royal Statistical Society, Series B (Methodological)*, vol. 76, pp. 373-397, 2014.
- [5] N. Friedman, "Inferring cellular networks using probabilistic graphical models," *Science*, vol 303, pp. 799-805, 2004.
- [6] S.L. Lauritzen and N.A. Sheehan, "Graphical models for genetic analyses," *Statistical Science*, vol. 18, pp. 489-514, 2003.
- [7] N. Meinshausen and P. Bühlmann, "High-dimensional graphs and variable selection with the Lasso," *Ann. Statist.*, vol. 34, no. 3, pp. 1436-1462, 2006.
- [8] K. Mohan, P. London, M. Fazel, D. Witten and S.I. Lee, "Node-based learning of multiple Gaussian graphical models," *J. Machine Learning Research*, vol. 15, pp. 445-488, 2014.
- [9] D.R. Brillinger, "Remarks concerning graphical models of times series and point processes," *Revista de Econometria (Brazilian Rev. Econometr.)*, vol. 16, pp. 1-23, 1996.
- [10] R. Dahlhaus, "Graphical interaction models for multivariate time series," *Metrika*, vol. 51, pp. 157-172, 2000.
- [11] U. Gather, M. Imhoff and R. Fried, "Graphical models for multivariate time series from intensive care monitoring," *Statistics in Medicine*, vol. 21, no. 18, 2002.
- [12] A. Abdelwahab, O. Amor and T. Abdelwahed, "The analysis of the interdependence structure in international financial markets by graphical models," *Int. Res. J. Finance Econ.*, pp. 291-306, 2008.
- [13] J. Songsiri, J. Dahl and L. Vandenberghe, "Graphical models of autoregressive processes," in Y. Eldar and D. Palomar (eds.), *Convex Optimization in Signal Processing and Communications*, pp. 89-116, Cambridge, UK: Cambridge Univ. Press, 2009
- [14] J. Songsiri and L. Vandenberghe, "Topology selection in graphical models of autoregressive processes," *J. Machine Learning Res.*, vol. 11, pp. 2671-2705, 2010.
- [15] K. Khare, S.-Y. Oh and B. Rajaratnam, "A convex pseudolikelihood framework for high dimensional partial correlation estimation with convergence guarantees," *J. Royal Statistical Society: Statistical Methodology, Series B*, vol. 77, Part 4, pp. 803-825, 2015.
- [16] A. Goldenberg, A.X. Zheng, S.E. Fienberg and E.M. Airolidi, "A survey of statistical network models," *Foundations and Trends in Machine Learning*, vol. 2, no. 2, pp. 129-233, 2009.
- [17] T. Medkour, A.T. Walden, A.P. Burgess, and V.B. Strelets, "Brain connectivity in positive and negative syndrome schizophrenia," *Neuroscience*, vol. 169, no. 4, pp. 1779-1788, 2010.
- [18] R.J. Wolstenholme and A.T. Walden, "An efficient approach to graphical modeling of time series," *IEEE Trans. Signal Process.*, vol. 64, no. 12, pp. 3266-3276, June 15, 2015.
- [19] D. Schneider-Luftman, "p-Value combiners for graphical modelling of EEG data in the frequency domain," *J. Neuroscience Methods*, vol. 271, pp. 92-106, 2016.
- [20] G. Marrelec, A. Krainik, H. Duffau, M. Pélégrini-Issac, M.S. Lehericy, J. Doyon and H. Benali, "Partial correlation for functional brain interactivity investigation in functional MRI," *NeuroImage*, vol. 32, pp. 228-237, 2006.
- [21] S. Ryali, T. Chen, K. Supekar and V. Menon, "Estimation of functional connectivity in fMRI data using stability selection-based sparse partial correlation with elastic net penalty," *NeuroImage*, vol. 59, pp. 3852-3861, 2012.
- [22] A.J. Rothman, P.J. Bickel, E. Levina and J. Zhu, "Sparse permutation invariant covariance estimation," *Electronic J. Statistics*, vol. 2, pp. 494-515, 2008.
- [23] C. Lam and J. Fan, "Sparsistency and rates of convergence in large covariance matrix estimation," *Ann. Statist.*, vol. 37, no. 6B, pp. 4254-4278, 2009.
- [24] Y. Matsuda, "A test statistic for graphical modelling of multivariate time series," *Biometrika*, vol. 93, no. 2, pp. 399-409, 2006.
- [25] J.K. Tugnait, "Edge exclusion tests for graphical model selection: Complex Gaussian vectors and time series," *IEEE Trans. Signal Process.*, vol. 67, no. 19, pp. 5062-5077, Oct. 1, 2019.
- [26] M. Eichler, "Graphical modelling of dynamic relationships in multivariate time series," in B. Schelter, M. Winterhalder and J. Timmer (eds.), *Handbook of time series analysis: Recent theoretical developments and applications*, pp. 335-372, New York: Wiley-VCH, 2006.
- [27] M. Eichler, "Graphical modelling of multivariate time series," *Probability Theory and Related Fields*, vol. 153, issue 1-2, pp. 233-268, June 2012.
- [28] A. Jung, R. Heckel, H. Bölcskei, and F. Hlawatsch, "Compressive nonparametric graphical model selection for time series," in *Proc. IEEE ICASSP-2014*, Florence, Italy, May 2014.
- [29] A. Jung, "Learning the conditional independence structure of stationary time series: A multitask learning approach," *IEEE Trans. Signal Process.*, vol. 63, no. 21, pp. 5677-5690, Nov. 1, 2015.
- [30] A. Jung, G. Hannak and N. Goertz, "Graphical LASSO based model selection for time series," *IEEE Signal Process. Lett.*, vol. 22, no. 10, pp. 1781-1785, Oct. 2015.
- [31] A. Tank, N.J. Foti and E.B. Fox, "Bayesian structure learning for stationary time series," in *Proc. UAI '15 (31st Conf. Uncertainty in Artificial Intelligence)*, Amsterdam, July 12-16, 2015, pp. 872-881.
- [32] N.J. Foti, R. Nadkarni, A.K.C. Lee and E.B. Fox, "Sparse plus low-rank graphical models of time series for functional connectivity in MEG," in *Proc. 2nd SIGKDD Workshop on Mining and Learning from Time Series*, 2016.
- [33] N. Tran, O. Abramenko and A. Jung, "On the sample complexity of graphical model selection from non-stationary samples," *IEEE Trans. Signal Process.*, vol. 68, pp. 17-32, 2020
- [34] D.R. Brillinger, *Time Series: Data Analysis and Theory*, Expanded edition. New York: McGraw Hill, 1981.
- [35] F.R. Bach and M.I. Jordan, "Learning graphical models for stationary time series," *IEEE Trans. Signal Process.*, vol. 52, no. 8, pp. 2189-2199, Aug. 2004.
- [36] P. Whittle, "The analysis of multiple stationary time series," *J. Royal Statistical Society: Statistical Methodology, Series B*, vol. 15, no. 1, pp. 125-139, 1953.
- [37] J.K. Tugnait, "Graphical modeling of high-dimensional time series," in *Proc. 52nd Asilomar Conference on Signals, Systems and Computers*, pp. 840-844, Pacific Grove, CA, Oct. 29 - Oct. 31, 2018.
- [38] J.K. Tugnait, "Consistency of sparse-group lasso graphical model selection for time series," *Proc. 54th Asilomar Conference on Signals, Systems and Computers*, Pacific Grove, CA, Nov. 1-4, 2020, pp. 589-593.

- [39] J.K. Tugnait, "On sparse complex Gaussian graphical model selection," in *Proc. 2019 IEEE Intern. Workshop on Machine Learning for Signal Processing (MLSP 2019)*, Pittsburgh, PA, Oct. 13-16, 2019.
- [40] G. Casella and R.L. Berger, *Statistical Inference*, 2nd edition. Pacific Grove, CA: Duxbury, 2002.
- [41] P.J. Schreier and L.L. Scharf, *Statistical Signal Processing of Complex-Valued Data*, Cambridge, UK: Cambridge Univ. Press, 2010.
- [42] N. Simon, J. Friedman, T. Hastie and R. Tibshirani, "A sparse-group lasso," *J. Computational Graphical Statistics*, vol. 22, pp. 231-245, 2013.
- [43] J. Friedman, T. Hastie and R. Tibshirani, "A note on the group lasso and a sparse group lasso," *arXiv:1001.0736v1 [math.ST]*, 5 Jan 2010.
- [44] J.K. Tugnait, "Sparse-group lasso for graph learning from multi-attribute data," *IEEE Trans. Signal Process.*, vol. 69, pp. 1771-1786, 2021.
- [45] A. Hjørungnes and D. Gesbert, "Complex-valued matrix differentiation: techniques and key results," *IEEE Trans. Signal Processing*, vol. 55, no. 6, pp. 2740-2746, June 2007.
- [46] L. Li, X. Wang and G. Wang, "Alternating direction method of multipliers for separable convex optimization of real functions in complex variables," *Mathematical Problems in Engineering*, vol. 2015, Article ID 104531, 14 pages, <http://dx.doi.org/10.1155/2015/104531>
- [47] E. Ollila, "Direction of arrival estimation using robust complex Lasso," in *Proc. 2016 10th European Conf. Antennas Propag. (EuCAP)*, Davos, April 2016, pp. 1-5.
- [48] S. Boyd, N. Parikh, E. Chu, B. Peleato and J. Eckstein, "Distributed optimization and statistical learning via the alternating direction method of multipliers," *Foundations and Trends in Machine Learning*, vol. 3, no. 1, pp. 1-122, 2010.
- [49] P. Ravikumar, M.J. Wainwright, G. Raskutti and B. Yu, "High-dimensional covariance estimation by minimizing ℓ_1 -penalized log-determinant divergence," *Electronic J. Statistics*, vol. 5, pp. 935-980, 2011.
- [50] J. Dattorro, *Convex Optimization & Euclidean Distance Geometry*. Palo Alto, CA: Meboo Publishing, 2013.
- [51] K.B. Petersen and M.S. Pedersen, "The matrix cookbook," 2012. [Online]. Available: <http://www2.imm.dtu.dk/pubdb/p.php?3274>.